UC Santa Cruz

UC Santa Cruz Electronic Theses and Dissertations

Title

An order-to-disorder structural switch activates the FoxM1 transcription factor

Permalink

https://escholarship.org/uc/item/8zw6f5x2

Author

Brison, Caileen Marie

Publication Date

2019

Peer reviewed|Thesis/dissertation

eScholarship.org Powered by the California Digital Library
University of California

University of California
Santa Cruz

An order-to-disorder structural switch activates the FoxM1 transcription factor

A dissertation submitted in partial satisfaction of the requirements for the degree of

DOCTOR OF PHILOSOPHY

in

CHEMISTRY

by

Caileen M. Brison

June 2019

The dissertation of Caileen M. Brison is approved:

_____
Professor Seth Rubin, chair

_____
Professor Doug Kellogg

_____
Professor Glenn Millhauser

_____
Associate Professor Carrie Partch

_____
Quentin Williams
Acting Vice Provost and Dean of Graduate Studies

Copyright © by
Caileen M Brison
2019

Table of Contents **Page**

List of Figures……vi

List of Tables……vi

Abstract……...vii

Acknowledgements……..……..……..…viii

Chapter 1: FoxM1 transcriptional regulation and the cell cycle

1.1 Introduction……1

1.1.1 The cell cycle and cancer……..……1

1.1.2 The G2/M transition……2

1.1.3 The role of FoxM1 in the cell cycle……2

1.1.4 FoxM1 is comprised primarily of intrinsic disorder…….....5

1.1.5 FoxM1 domain architecture…….....6

1.1.6 FoxM1 regulatory interactions with CBP……..7

1.1.7 FoxM1 is a substrate of Cyclin-dependent kinases and Polo-like kinase 1…8

1.1.8 Conclusions……...9

1.2 References……10

Chapter 2: Phosphorylation of FoxM1 dictates association with regulatory partners

2.1 Introduction……..……..……..……..……..……...15

2.2 Results……..……..……..……..……16

2.2.1 FoxM1 NRD directly binds the TAD……16

2.2.2 FoxM1 TAD directly binds co-activator CBP……..17

2.2.3 FoxM1 TAD cannot simultaneously bind multiple domains of CBP…...……17

2.2.4 CBP cannot bind auto-repressed FoxM1……20

2.2.5 Cdk phosphorylation has no direct effect on NRD-TAD binding…….22

2.2.6 Cdk phosphorylation has no effect on CBP binding to FoxM1……22

2.2.7. Plk phosphorylation has no effect on CBP binding to FoxM1……..23

2.2.8. Plk1 phosphorylation obliterates NRD binding……...24

2.2.9. Cdk phosphorylation of the CSR allows Plk1 polobox binding domain association……25

2.2.10. Conclusions……26

2.3 Discussion……27

2.4 Materials and Methods……27

2.4.1 Protein Expression ……27

2.4.2 Isothermal titration calorimetry……28

2.4.3 Kinase reactions……29

2.4.4 Cell culture……30

2.4.5 NMR sample prep……31

2.5 References……32

Chapter 3: Chapter 3: FoxM1 structural confirmations and dynamics

3.1 Introduction……34

3.2 Results……35

3.2.1. The FoxM1 TAD has intrinsic disorder and partially globular domains…….35

3.2.2 FoxM1 NRD-TAD structural model…….....36

3.2.3 The NRD-TAD has a hydrophobic core and disruption of the interface leads to heightened transcriptional activity…….....41

3.2.4 Disruption of CBP binding motif leads to decreased relief of repression…..43

3.2.5. FoxM1 TAD bound to CBP by NMR……43

3.2.6. The FoxM1 TAD has α-helical propensity in a CBP bound state……47

3.2.7. FoxM1 TAD is unstructured in a phosphorylated state……..49

3.2.8. Conclusions……50

3.3 Discussion……52

3.4 Materials and Methods……55

3.4.1 Protein expression……55

3.4.2 Circular dichroism……55

3.4.3 Protein expression for NMR……55

3.4.4 Nuclear magnetic resonance data collection and assignments……56

3.4.5 Structure modeling using RASREC-Rosetta……58

3.4.6 Cell culture……60

3.4.7 Western blot and cell cycle analysis……61

3.5 References……63

List of Figures **Page**

Chapter 1

Figure 1.1: FoxM1 is a key regulator of the G2/M transition……4

Figure 1.2: FoxM1 domain architecture and phosphorylation sites……9

Chapter 2

Figure 2.1: FoxM1 NRD directly binds the TAD *in vitro*……..……..……...17

Figure 2.2: FoxM1 binds CBP……..……..19

Figure 2.3: CBP cannot bind auto-repressed FoxM1……21

Figure 2.4: Cdk phosphorylation has no direct role in regulation of FoxM1 interactions.……23

Figure 2.5: Phosphorylation of the TAD by Plk1 regulates NRD-TAD interactions……...25

Figure 2.6: Plk1 polobox binding domain binds Cdk phosphorylated CSR……..……26

Chapter 3

Figure 3.1: FoxM1 NRD and TAD are intrinsically disordered……..……..36

Figure 3.2: Solution structure of NRD-TAD complex……..……38

Figure 3.3: Interactions stabilizing the NRD-TAD hydrophobic core and interface..……41

Figure 3.4: The FoxM1 TAD and CBP by NMR……46

Figure 3.5: CBP bound TAD shows α-helical propensity……..……48

Figure 3.6: The Plk1 phosphorylated TAD is intrinsically disordered……..……50

List of Tables

Chapter 3

Table 3.1: FoxM1 TAD bound by CBP-TAZ2 chemical shift assignments……45

Abstract

An order-to-disorder structural switch activates the FoxM1 transcription factor

Caileen M. Brison

Intrinsically disordered transcription factor transactivation domains (TADs) function through structural plasticity, adopting ordered conformations when bound to transcriptional co-regulators. Many transcription factors contain a negative regulatory domain (NRD) that suppresses recruitment of transcriptional machinery through autoregulation of the TAD. We report the solution structure of an autoinhibited NRD-TAD complex within FoxM1, a critical activator of mitotic gene expression. We observe that while both the FoxM1 NRD and TAD are primarily intrinsically disordered domains, they associate and adopt a structured conformation. We identify how Plk1 and Cdk kinases cooperate to phosphorylate FoxM1, which releases the TAD into a disordered conformation that then associates with the TAZ2 or KIX domains of the transcriptional co-activator CBP. Our results support a mechanism of FoxM1 regulation in which the TAD undergoes switching between disordered and different ordered structures.

Acknowledgements

I'd like to first and foremost thank my parents, Arland and John Dorais, for their continued support throughout my educational career and otherwise. They have allowed me to explore and remain curious about my own life in its entirety and for that I am grateful. I would also like to thank my P.I. Dr. Seth Rubin who has guided me through my PhD and significantly aided in my scientific progression. Without Seth I don't think I would have grasped the critical importance of being an independent yet collaborative investigator. I would also like to thank my committee, Dr. Carrie Partch, Dr. Doug Kellogg, and Dr. Glenn Millhauser for their continued academic guidance. In specific, I'd like to thank Dr. Carrie Partch who has been instrumental in my navigation of graduate school. Carrie helped shape my scientific communication, analysis, and taught me much of what I know about NMR. In addition, I would like to thank my friend, mentor, and co-author Dr. Aimee Marceau for her guidance, support, and collaboration throughout this work. Without her efforts none of this would be possible. I also want to thank my lab mates current and past for creating a wonderful work environment and contributing to the overall scientific rigor of the department. I also need to thank the Partch Lab past and present for their scientific contributions and help in experimental design, specifically Dr. Jennifer Fribourgh, Dr. Efrain Ceh Pavia, Dr. Alicia Michael, and Dr. Stacy Harvey. I would also like to thank my core group of friends, Dr. Jessica Morgan Garcia, Dr. Linnea Jansson, and Jolene Draper. These women have been critical for my during graduate school and my time in California and without them I would have had a very different graduate school experience. I also need to thank the Center for Innovations in Teaching and Learning as well as the Women's Center for their continued support and resources as well as the Chemistry Department and the Graduate Division, specifically Janet Jones, Karen Meece, Dr. Ilan Benjamin, and Katie Cramton.

Chapter 1 – FoxM1 transcriptional regulation and the cell cycle

1.1. Introduction

1.1.1. The cell cycle and cancer

The cell cycle is a tightly coordinated and highly conserved process that ensures cell fidelity across organisms. The maintenance of the cell cycle is critical for the life of an organism and disruption of this cell cycle can prove fatal. During development, cells are consistently dividing and differentiating. Once cells become terminally differentiated, they are no longer cycling. If cells acquire cancerous mutagens, the cell cycle can be reactivated in a manner that is deregulated and the subsequent consequence is tumorigenesis and cancer. Thusly, understanding the cell cycle is crucial not only for developmental biology, but cancer biology as well.

The cell cycle can be thought of in four primary phases that are separated by distinct transitions. The cell cycle consists of two growth phases (G_1 and G_2) – or gap phases – that separate a mitotic phase (M) and a DNA synthesis phase (S). In addition to cells undergoing cell division via the mitotic process, cells can also temporarily exit the cell cycle and go into a state of quiescence (G_0) whereby the cells are no longer cycling.

The deregulation of proper cell cycle is a hallmark of cancer biology and understanding the regulation of the cell cycle is not only critical for developmental biology but cancer biology as well. The role of cell cycle proteins in cancer biology and as potential cancer targets has been demonstrated by numerous studies and reviewed at length (Otto and Sicinski 2017; Hanahan and Weinberg 2000). The proper progression of the cell cycle is regulated in large part by transcription factors that coordinate the expression of cell cycle genes and ensure fidelity across the transitions between cell cycle phases. One of the key transitions in late stage cell cycle in the G2/M transition. The G2/M transition is critical as the passage of the transition prepares the cell for irreversible division.

1.1.2. The G2/M transition

The G2/M transition is initiated by Cdk/cyclin complexes early in G1 stage and the core mechanism is conserved from yeast to humans (Swaffer et al. 2016; Murakami et al. 2010; Pines 1995; Toyoshima et al. 1998). The phosphorylation of Cdk1/cyclin b by Cyclin-dependent kinases (Cdks), Plk (Polo-like kinase), and Ckd-activating kinase (CAK) in humans helps drive the mitotic cell cycle. In contrast to these activating phosphorylation marks, the G2/M transition is inhibited by phosphorylation as Wee1 and Myt1 phosphorylation activity on Cdk/cyclin complexes hault cell cycle progression (Fesquet et al. 1993, 161; Poon et al. 1993; Murakami et al. 2010; Golsteyn et al., n.d.). Counteracting dephosphorylation on Cdk/cyclin complexes by CDC25 ensures proper temporal regulation of Cdk/cyclin phosphorylation and thusly cell cycle progression (Russell and Nurse 1986, 25; Sanchez et al. 1997, 25).

The G2/M transition is also marked by an increase in late cell cycle genes and their subsequent activity, of note the heightened expression of Forkhead Box M1 (FoxM1) (Müller et al. 2016). In addition to kinase activity, gene expression patterns and transcriptional activity tightly regulate the G2/M transition. FoxM1 expression begins to rise as the cell cycle progresses from the G1 phase to the G2/M transition. This increase in FoxM1 levels and activity is concurrent with an overall increase in late cell cycle genes which is a direct consequence of early cell cycle regulation by the aforesaid (X. Chen et al. 2013, 1; Jamila Laoukili et al. 2005, 1; Wonsey and Follettie 2005, 1; Müller et al. 2016; X. Chen et al. 2013). This temporal regulation via phosphorylation is critical for cell cycle fidelity and the role of phosphorylation on FoxM1 will be detailed in this work.

1.1.3 The role of FoxM1 in the cell cycle

The passage of the G2/M transition is coordinated by cell cycle genes under the control of E2F, CDE, and CHR promoters as well as forkhead box (FOX) transcription factors which bind to a conserved FKH motif and are also recruited to CHR promoters (Müller et al.

2016; X. Chen et al. 2013). There are approximately 50 FOX proteins in the human genome that are categorized as such due to conservation of their winged helix DNA binding domain (Jackson et al. 2010). Of interest to the G2/M transition is the transcription factor Forkhead Box M1 (FoxM1) which controls cell cycle genes and is required for proper development, mitotic entry, and proper execution of the mitotic program (W Korver, Roose, and Clevers 1997; Wouter Korver et al. 1998; Jamila Laoukili et al. 2005; I.-C. Wang et al. 2005; Wonsey and Follettie 2005). Throughout the cell cycle and leading towards full activation of FoxM1 we see a rise in Cyclin-dependent kinase (Cdk) activity beginning in G1 (J. Laoukili et al. 2008; Anders et al. 2011; Lüscher-Firzlaff, Lilischkis, and Lüscher 2006). This Cdk activity is critical for FoxM1 as we will discuss in detail. The activity of Cdks across the G1/S transition is subsequently followed by expression of FoxM1 and Polo-like kinase 1 (Plk1) as we progress towards G2 (Fu et al. 2008). The levels of FoxM1 and Plk1 peak across the G2/M transition and this coordinated expression aids in the passage of the G2/M transition and marks complete activation of FoxM1 and the expression of the FoxM1 genes in the mitotic program (J. Laoukili et al. 2008, 2) (Figure 1.1). FoxM1 expression is typically confined to dividing cells and is required for embryogenesis, hematopoiesis, and tissue repair (Wouter Korver et al. 1998; Ramakrishna et al. 2007; Ustiyan et al. 2009). FoxM1 is essential for proper development; null mice exhibit an embryonic lethal phenotype due to liver, blood, heart, and lung abnormalities resulting from proliferation defects (Ramakrishna et al. 2007).

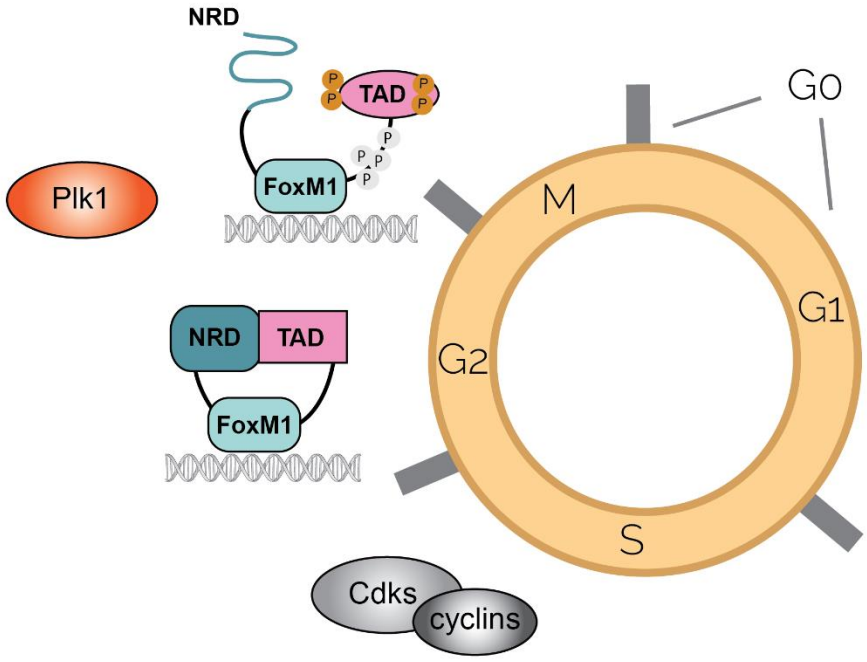


Figure 1.1: FoxM1 is a key regulator of the G2/M transition in the cell cycle. The cell cycle consists of the four primary phases; growth phase 1 (G1), growth phase 2 (G2), mitosis (M), and DNA synthesis (S). Cells can also exit the cell cycle and go into a state of non - cycling (G0). Cdk expression levels begin to rise across the G1/S transition and we begin to see presumably inactive FoxM1 expression. As FoxM1 levels rise, Plk1 levels rise in a positive feedback loop, further phosphorylating FoxM1 with peak levels of fully phosphorylated FoxM1 across the G2/M transition.

Alongside FoxM1's critical role in cell cycle biology and development, we see FoxM1 activity deregulated in all well characterized and studied cancers (Koo, Muir, and Lam 2012; Millour et al. 2010; Myatt and Lam 2007). FoxM1 misregulation at both the transcriptional and protein level has been observed in adenocarcinomas, breast cancer, squamous cell carcinomas, leukemia, lymphoma, and many additional malignancies (Kwok et al. 2010; Millour et al. 2010; Hyun Jung Park et al. 2011; Ramakrishna et al. 2007). Several studies have shown that FoxM1 activates tumor metastasis, mediates drug resistance, and regulates pluripotency-associated genes responsible for maintaining tumor cells in their undifferentiated state (Carr et al. 2010; Kwok et al. 2010; Z. Wang et al. 2011; Hyun Jung Park et al. 2011). Additionally, deletion of FoxM1 in cancer cells inhibits tumor development and growth and

leads to increased apoptosis (Kalinichenko et al. 2004; Wonsey and Follettie 2005). Due to the relevance of FoxM1 in proper development and the deregulation of FoxM1 in cancer cells, understanding the mechanism of activation and repression is crucial for cell cycle biology. In addition, detailing a structural and mechanistic profile of FoxM1 could also provide a platform for cancer specific biomolecular drug targets.

1.1.4. FoxM1 is comprised primarily of intrinsic disorder

FoxM1 – as well as many eukaryotic transcription factors – are comprised primarily of intrinsically disordered regions (Liu et al. 2006; Babu et al. 2011). Intrinsically disordered proteins (IDPs) or intrinsically disordered regions (IDRs) have become widely recognized as critical regulatory mechanisms of biological processes, specifically eukaryotic transcription and cellular signaling. Common mechanisms of transcriptional control by IDRs and IDPs is often a “folding upon binding” significant structural rearrangement and/or a small disordered region terminal to a globular domain gaining structure upon binding. A common and relevant example of these mechanisms is the folding of disordered TADs upon binding to CBP domains. (Xu et al. 2015; Ebert et al. 2008; Goto et al. 2002; F. Wang et al. 2012)These regions of intrinsic disorder give rise to the function of these transcription factors and allows for plasticity in structure (Minezaki et al. 2006; Dyson and Wright 2005). Eukaryotic transcription factors have been well characterized to have large regions of disorder that adopt order upon binding to partners (Wright and Dyson 2015; Liu et al. 2006). These regulatory mechanism gives rise to the ability of transcription factors to fulfill complex biological roles that require flexibility in their binding capacities. As such, the investigations of eukaryotic transcription factors through the lens of disorder provides important insight regarding function.

Outside of the winged-helix DNA binding domain, FoxM1 is expected to be primarily unstructured based on primary sequence analysis (Littler et al. 2010). Predictions for disorder for Forkhead Box proteins have been reported to be approximately 70% on average

(Minezaki et al. 2006). Due to the large presence of disorder within FoxM1 and it's critical role in cell cycle biology, understanding the role of disorder in this transcription factor is critical for our understanding of function. The domain architecture of FoxM1 is defined by functional portions of the protein that have been shown to have critical relevance to the overall transcriptional properties of FoxM1, notable the N-terminal repressive domain and the transactivation domain. However, despite the relevance of these domains, very little is known of FoxM1s structural properties outside of the DNA binding domain.

1.1.5. FoxM1 domain architecture

FoxM1 has an N-terminal regulatory domain (NRD), a winged helix DNA binding domain (DBD), a region of high Cdk consensus sites called the 'Cdk site region' (CSR) and a transactivation domain. In functional assays to assess transcription, removal of the NRD leads to constitutively active FoxM1 as monitored by luciferase activity and has been proposed to inhibit FoxM1 activity by sequestration of the TAD (H J Park et al. 2008). The NRD has one Cdk phosphorylation site (J. Laoukili et al. 2008). The DBD has conserved winged-helix DNA binding motif. The DBD is the unifying domain across all Forkhead family proteins and is highly conserved and structured. The FoxM1 DBD domain has been crystallized in complex with a consensus Forkhead DNA motif (Littler et al. 2010). The CSR is a region in FoxM1 named so for a high frequency of Cdk phosphorylation sites (Anders et al. 2011; Lüscher-Firzlaff, Lilischkis, and Lüscher 2006; Kalinichenko et al. 2004; Y.-J. Chen et al. 2009, 1). Previous literature has not identified the CSR as a unique domain of FoxM1, however we see it has unique functional significance as will be demonstrated throughout this dissertation. Previous literature referred to the FoxM1 TAD as all residues C-terminal of the DBD. Here we clarify that region into distinct functional domains and identify a minimal TAD. The TAD is the most C-terminal fragment of FoxM1 and this region has been determined to have transcriptional activity as a domain (Littler et al. 2010; Shi, Kroeger, and Morimoto 1995; Wierstra and Alves 2006). The TAD of FoxM1 contains four Plk1 phosphorylation sites.

Despite the characterization of the functionality of domains, outside of the DBD very little is known about FoxM1 structure or dynamics.

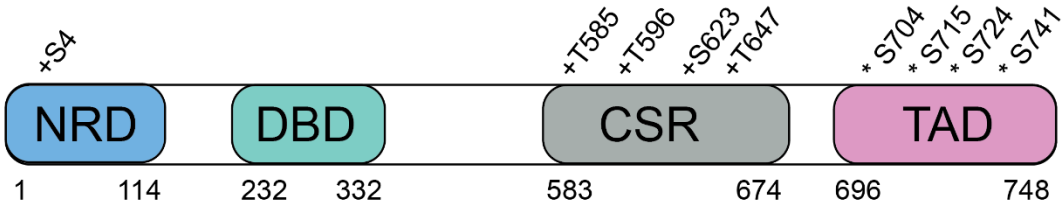


Figure 1.2: FoxM1 domain architecture and phosphorylation sites. Human FoxM1b isoform is a 748 amino acid transcription factor. FoxM1 has an N-terminal repressive domain (NRD), a winged-helix DNA binding domain (DBD), a Cdk site region (CSR), and a transactivation domain (TAD). Cdk phosphorylation sites are noted with a plus (+) and Plk1 phosphorylation sites are noted with an asterisk (*). Domain boundaries are noted below the architecture diagram.

1.1.6. FoxM1 regulatory interactions with CBP

Studies have proposed that FoxM1 NRD sequesters it's own TAD thus limiting transcriptional activity (J. Laoukili et al. 2008; Wierstra and Alves 2006; H J Park et al. 2008). TAD sequestration via an NRD in a common mechanism of repression among transcription factors and is critical for proper transcriptional regulation (Kim et al. 1999; H J Park et al. 2008; Wierstra and Alves 2006; Shi, Kroeger, and Morimoto 1995; Spengler and Brattain 2006). In addition, data show that FoxM1 Co-IPs with transcriptional co-activator CREB-binding protein (CBP) (Major, Lepe, and Costa 2004). CBP is a common co-activator and is widely implicated in transcriptional activation through it's ability to modify chromatin (Ogryzko et al. 1996; Kasper et al. 2006). CBP also has been shown to interact with numerous eukaryotic transcription factors to modulate and enhance their transcriptional activity (Major, Lepe, and Costa 2004; Mujtaba et al. 2004; Ogryzko et al. 1996). CBP is a large multi domain protein that also contains multiple domains that help facilitate protein:protein interactions. The protein:protein interaction domains of CBP are critical as they can help provide specificity to an otherwise nonspecific transcription factor. This is proposed to be pertinent within FoxM1 in particular which has been shown to have a very nonspecific binding pattern to DNA within the

genome (Sanders et al. 2015; X. Chen et al. 2013). Thusly, CBP can act as a liaison between transcription factors and the general transcription machinery while also enhancing transcription factor specificity. Among these protein:protein interaction domains are the zinc finger binding domains, TAZ1, TAZ2 and ZZ, the KIX domain, the nuclear receptor like coactivator binding domain (NCBD) domain, and the bromodomain (BRD) domain (De Guzman et al. 2006; Goto et al. 2002; I. Radhakrishnan et al. 1997; Mujtaba et al. 2004; De Guzman et al. 2000, 1). Due to the association between CBP and FoxM1 in a cell cycle dependent manner and the proposed mechanism of specificity, understanding the mechanism of FoxM1 activation is critical for out understanding of cancer biology.

1.1.7. FoxM1 is a substrate of Cyclin-dependent kinases and Polo-like kinase 1

FoxM1 is also a highly modified transcription factor and is a substrate of numerous kinases, of note here are the Cyclin dependent kinase (Cdk) family and Polo-like-1 (Plk1) kinase (J. Laoukili et al. 2008; Fu et al. 2008; Joshi et al. 2013). FoxM1 has long been known as a Cdk substrate and indeed we see as we transition from S phase through the G2/M transition we see a coordinated rise in Cdk activity on FoxM1 as well as an increase in FoxM1 transcriptional activity (Major, Lepe, and Costa 2004; J. Laoukili et al. 2008; Anders et al. 2011; Lüscher-Firzlaff, Lilischkis, and Lüscher 2006). While most of the literature indicates the Cdk activity is the primary driver of FoxM1 activation, phospo-specific antibody immunoblots and luciferase data show that FoxM1 is indeed a substrate of Plk1 and that FoxM1 activity increases as Plk1 concentration is increased in a dose-dependent manner (Fu et al. 2008). These data taken together indicate that both Cdk and Plk1 play a critical role in FoxM1 activation, yet we still do not understand the exact mechanism by which these kinases lead to FoxM1 activity.

1.1.8. Conclusions

FoxM1 is a key regulator of the cell cycle and a prominent oncogene across all well characterized cancers (W Korver, Roose, and Clevers 1997; Wouter Korver et al. 1998; Kalinichenko et al. 2004, 1; Carr et al. 2010; Raychaudhuri and Park 2011). Despite critical roles as both a transcription factor and oncogene very little is known about the mechanistic details of FoxM1. This is likely due to a high frequency of intrinsically disordered regions (IDRs) within FoxM1 and forkhead box proteins overall and the inherent challenge of working with IDRs *in vitro* (Minezaki et al. 2006). While FoxM1 has been targeted as a cancer therapeutic, the current targets are limited by a lack of detailed mechanism as well as off target effects as a consequence of targeting DNA binding ability (Gormally et al. 2014; S. K. Radhakrishnan et al. 2006). FoxM1 activity is directly associated with Cdk activity and Plk1 activity and the subsequent phosphorylation state of FoxM1. This dissertation shows that Cdk and Plk1 play unique yet interdependent roles in the ultimate de-repression of FoxM1. This relief of repression highlights the plasticity of FoxM1 structure as FoxM1 navigate between alternative confirmations dependent on the associated binding partner. Investigating oncogenic eukaryotic transcription factors in the context of the cell cycle provides deep insight towards potential cancer targets. This dissertation aims to give context to the ways in which FoxM1 is regulated in a phosphorylation dependent manner. This work can be used to guide the design of cancer therapeutics that specifically target FoxM1.

1.2. References

Anders, Lars, Nan Ke, Per Hydbring, Yoon J. Choi, Hans R. Widlund, Joel M. Chick, Huili Zhai, et al. 2011. “A Systematic Screen for CDK4/6 Substrates Links FOXM1 Phosphorylation to Senescence Suppression in Cancer Cells.” *Cancer Cell* 20 (5): 620–34.

Babu, M Madan, Robin van der Lee, Natalia Sanchez de Groot, and Jörg Gsponer. 2011. “Intrinsically Disordered Proteins: Regulation and Disease.” *Current Opinion in Structural Biology* 21 (3): 432–40.

Carr, Janai R., Hyun Jung Park, Zebin Wang, Megan M. Kiefer, and Pradip Raychaudhuri. 2010. “FoxM1 Mediates Resistance to Herceptin and Paclitaxel.” *Cancer Research* 70 (12): 5054–63.

Chen, Xi, Gerd A. Müller, Marianne Quaas, Martin Fischer, Namshik Han, Benjamin Stutchbury, Andrew D. Sharrocks, and Kurt Engeland. 2013. “The Forkhead Transcription Factor FOXM1 Controls Cell Cycle-Dependent Gene Expression through an Atypical Chromatin Binding Mechanism.” *Molecular and Cellular Biology* 33 (2): 227–36.

Chen, Yi-Ju, Carmen Dominguez-Brauer, Zebin Wang, John M. Asara, Robert H. Costa, Angela L. Tyner, Lester F. Lau, and Pradip Raychaudhuri. 2009. “A Conserved Phosphorylation Site within the Forkhead Domain of FoxM1B Is Required for Its Activation by Cyclin-CDK1.” *Journal of Biological Chemistry* 284 (44): 30695–707.

De Guzman, Roberto N., Natalie K. Goto, H. Jane Dyson, and Peter E. Wright. 2006. “Structural Basis for Cooperative Transcription Factor Binding to the CBP Coactivator.” *Journal of Molecular Biology* 355 (5): 1005–13.
.
De Guzman, Roberto N, Hong Yu Liu, Maria Martinez-Yamout, H.Jane Dyson, and Peter E Wright. 2000. “Solution Structure of the TAZ2 (CH3) Domain of the Transcriptional Adaptor Protein CBP.” *Journal of Molecular Biology* 303 (2): 243–53.

Dyson, H. Jane, and Peter E. Wright. 2005. “Intrinsically Unstructured Proteins and Their Functions.” *Nature Reviews Molecular Cell Biology* 6 (3): 197–208.

Ebert, Marc-Olivier, Sung-Hun Bae, H. Jane Dyson, and Peter E. Wright. 2008. “NMR Relaxation Study of the Complex Formed between CBP and the Activation Domain of the Nuclear Hormone Receptor Coactivator ACTR.” *Biochemistry* 47 (5): 1299–1308.

Fesquet, D., J. C. Labbé, J. Derancourt, J. P. Capony, S. Galas, F. Girard, T. Lorca, J. Shuttleworth, M. Dorée, and J. C. Cavadore. 1993. “The MO15 Gene Encodes the Catalytic Subunit of a Protein Kinase That Activates Cdc2 and Other Cyclin-Dependent Kinases (CDKs) through Phosphorylation of Thr161 and Its Homologues.” *The EMBO Journal* 12 (8): 3111–21.

Fu, Zheng, Liviu Malureanu, Jun Huang, Wei Wang, Hao Li, Jan M. van Deursen, Donald J. Tindall, and Junjie Chen. 2008. “Plk1-Dependent Phosphorylation of FoxM1 Regulates a Transcriptional Programme Required for Mitotic Progression.” *Nature Cell Biology* 10 (9): 1076–82.

Golsteyn, Roy M, Sharon J Schultz, Jiri Bartek, Andrew Ziemiecki, Thomas Ried, and Erich A Nigg. n.d. “Cell Cycle Analysis and Chromosomal Localization of Human Plk1, a Putative Homologue of the Mitotic Kinases Drosophila Polo and Saccharomyces Cerevisiae Cdc5,” 9.

Gormally, Michael V., Thomas S. Dexheimer, Giovanni Marsico, Deborah A. Sanders, Christopher Lowe, Dijana Matak-Vinković, Sam Michael, et al. 2014. “Suppression of the FOXM1 Transcriptional Programme via Novel Small Molecule Inhibition.” *Nature Communications* 5 (1): 5165.
.
Goto, Natalie K., Tsaffrir Zor, Maria Martinez-Yamout, H. Jane Dyson, and Peter E. Wright. 2002. “Cooperativity in Transcription Factor Binding to the Coactivator CREB-Binding Protein (CBP): THE MIXED LINEAGE LEUKEMIA PROTEIN (MLL) ACTIVATION DOMAIN BINDS TO AN ALLOSTERIC SITE ON THE KIX DOMAIN.” *Journal of Biological Chemistry* 277 (45): 43168–74.

Hanahan, Douglas, and Robert A Weinberg. 2000. “The Hallmarks of Cancer.” *Cell* 100 (1): 57–70. https://doi.org/10.1016/S0092-8674(00)81683-9.

Joshi, Kaushal, Yeshavanth Banasavadi-Siddegowda, Xiaokui Mo, Sung-Hak Kim, Ping Mao, Cenk Kig, Diana Nardini, et al. 2013. “MELK-Dependent FOXM1 Phosphorylation Is Essential for Proliferation of Glioma Stem Cells.” *Stem Cells (Dayton, Ohio)* 31 (6): 1051–63.

Kalinichenko, Vladimir V., Michael L. Major, Xinhe Wang, Vladimir Petrovic, Joseph Kuechle, Helena M. Yoder, Margaret B. Dennewitz, et al. 2004. “Foxm1b Transcription Factor Is Essential for Development of Hepatocellular Carcinomas and Is Negatively Regulated by the P19ARF Tumor Suppressor.” *Genes & Development* 18 (7): 830–50.

Kasper, Lawryn H., Tomofusa Fukuyama, Michelle A. Biesen, Fayçal Boussouar, Caili Tong, Antoine de Pauw, Peter J. Murray, Jan M. A. van Deursen, and Paul K. Brindle. 2006. “Conditional Knockout Mice Reveal Distinct Functions for the Global Transcriptional Coactivators CBP and P300 in T-Cell Development.” *Molecular and Cellular Biology* 26 (3): 789–809.

Kim, W Y, M Sieweke, E Ogawa, H J Wee, U Englmeier, T Graf, and Y Ito. 1999. “Mutual Activation of Ets-1 and AML1 DNA Binding by Direct Interaction of Their Autoinhibitory Domains.” *The EMBO Journal* 18 (6): 1609–20.

Koo, Chuay-Yeng, Kyle W. Muir, and Eric W.-F. Lam. 2012. “FOXM1: From Cancer Initiation to Progression and Treatment.” *Biochimica et Biophysica Acta (BBA) - Gene Regulatory Mechanisms* 1819 (1): 28–37.

Korver, W, J Roose, and H Clevers. 1997. “The Winged-Helix Transcription Factor Trident Is Expressed in Cycling Cells.” *Nucleic Acids Research* 25 (9): 1715–19.

Korver, Wouter, Marco W. Schilham, Petra Moerer, Maurice J. van den Hoff, Klaas Dam, Wouter H. Lamers, René H. Medema, and Hans Clevers. 1998. “Uncoupling of S Phase and Mitosis in Cardiomyocytes and Hepatocytes Lacking the Winged-Helix Transcription Factor Trident.” *Current Biology* 8 (24): 1327-S1.

Kwok, Jimmy M.-M., Barrie Peck, Lara J. Monteiro, Helma D. C. Schwenen, Julie Millour, R. Charles Coombes, Stephen S. Myatt, and Eric W.-F. Lam. 2010. “FOXM1 Confers Acquired Cisplatin Resistance in Breast Cancer Cells.” *Molecular Cancer Research* 8 (1): 24–34.

Laoukili, J., M. Alvarez, L. A. T. Meijer, M. Stahl, S. Mohammed, L. Kleij, A. J. R. Heck, and R. H. Medema. 2008. “Activation of FoxM1 during G2 Requires Cyclin A/Cdk-Dependent Relief of Autorepression by the FoxM1 N-Terminal Domain.” *Molecular and Cellular Biology* 28 (9): 3076–87.

Laoukili, Jamila, Matthijs R. H. Kooistra, Alexandra Brás, Jos Kauw, Ron M. Kerkhoven, Ashby Morrison, Hans Clevers, and René H. Medema. 2005. “FoxM1 Is Required for Execution of the Mitotic Programme and Chromosome Stability.” *Nature Cell Biology* 7 (2): 126–36.

Littler, D. R., M. Alvarez-Fernández, A. Stein, R. G. Hibbert, T. Heidebrecht, P. Aloy, R. H. Medema, and A. Perrakis. 2010. “Structure of the FoxM1 DNA-Recognition Domain Bound to a Promoter Sequence.” *Nucleic Acids Research* 38 (13): 4527–38.

Liu, Jiangang, Narayanan B. Perumal, Christopher J. Oldfield, Eric W. Su, Vladimir N. Uversky, and A. Keith Dunker. 2006. “Intrinsic Disorder in Transcription Factors.” *Biochemistry* 45 (22): 6873–88.

Lüscher-Firzlaff, Juliane M., Richard Lilischkis, and Bernhard Lüscher. 2006. “Regulation of the Transcription Factor FOXM1c by Cyclin E/CDK2.” *FEBS Letters* 580 (7): 1716–22.

Major, M. L., R. Lepe, and R. H. Costa. 2004. “Forkhead Box M1B Transcriptional Activity Requires Binding of Cdk-Cyclin Complexes for Phosphorylation-Dependent Recruitment of P300/CBP Coactivators.” *Molecular and Cellular Biology* 24 (7): 2649–61.

Millour, J, D Constantinidou, A V Stavropoulou, M S C Wilson, S S Myatt, J M-M Kwok, K Sivanandan, et al. 2010. “FOXM1 Is a Transcriptional Target of ERα and Has a Critical Role in Breast Cancer Endocrine Sensitivity and Resistance.” *Oncogene* 29 (20): 2983–95.

Minezaki, Yoshiaki, Keiichi Homma, Akira R. Kinjo, and Ken Nishikawa. 2006. “Human Transcription Factors Contain a High Fraction of Intrinsically Disordered Regions Essential for Transcriptional Regulation.” *Journal of Molecular Biology* 359 (4): 1137–49.

Mujtaba, Shiraz, Yan He, Lei Zeng, Sherry Yan, Olga Plotnikova, Sachchidanand, Roberto Sanchez, Nancy J Zeleznik-Le, Ze’ev Ronai, and Ming-Ming Zhou. 2004. “Structural Mechanism of the Bromodomain of the Coactivator CBP in P53 Transcriptional Activation.” *Molecular Cell* 13 (2): 251–63.

Müller, Gerd A., Konstanze Stangner, Thomas Schmitt, Axel Wintsche, and Kurt Engeland. 2016. “Timing of Transcription during the Cell Cycle: Protein Complexes Binding to E2F, E2F/CLE, CDE/CHR, or CHR Promoter Elements Define Early and Late Cell Cycle Gene Expression.” *Oncotarget* 8 (58): 97736–48.

Murakami, Hiroshi, Hirofumi Aiba, Makoto Nakanishi, and Yuko Murakami-Tonami. 2010. “Regulation of Yeast Forkhead Transcription Factors and FoxM1 by Cyclin-Dependent and Polo-like Kinases.” *Cell Cycle* 9 (16): 3253–62.

Myatt, Stephen S., and Eric W. -F. Lam. 2007. “The Emerging Roles of Forkhead Box (Fox) Proteins in Cancer.” *Nature Reviews Cancer* 7 (11): 847–59.

Ogryzko, Vasily V, R. Louis Schiltz, Valya Russanova, Bruce H Howard, and Yoshihiro Nakatani. 1996. “The Transcriptional Coactivators P300 and CBP Are Histone Acetyltransferases.” *Cell* 87 (5): 953–59.

Otto, Tobias, and Piotr Sicinski. 2017. “Cell Cycle Proteins as Promising Targets in Cancer Therapy.” *Nature Reviews. Cancer* 17 (2): 93–115.

Park, H J, Z Wang, R H Costa, A Tyner, L F Lau, and P Raychaudhuri. 2008. “An N-Terminal Inhibitory Domain Modulates Activity of FoxM1 during Cell Cycle.” *Oncogene* 27 (12): 1696–1704.

Park, Hyun Jung, Galina Gusarova, Zebin Wang, Janai R. Carr, Jing Li, Ki-Hyun Kim, Jin Qiu, et al. 2011. “Deregulation of FoxM1b Leads to Tumour Metastasis: FoxM1, a Metastasis Factor.” *EMBO Molecular Medicine* 3 (1): 21–34.

Pines, J. 1995. “Cyclins and Cyclin-Dependent Kinases: A Biochemical View.” *Biochemical Journal* 308 (3): 697–711.

Poon, R. Y., K. Yamashita, J. P. Adamczewski, T. Hunt, and J. Shuttleworth. 1993. “The Cdc2-Related Protein P40MO15 Is the Catalytic Subunit of a Protein Kinase That Can Activate P33cdk2 and P34cdc2.” *The EMBO Journal* 12 (8): 3123–32.

Radhakrishnan, Ishwar, Gabriela C. Pérez-Alvarado, David Parker, H. Jane Dyson, Marc R. Montminy, and Peter E. Wright. 1997. “Solution Structure of the KIX Domain of CBP Bound to the Transactivation Domain of CREB: A Model for Activator:Coactivator Interactions.” *Cell* 91 (6): 741–52.

Radhakrishnan, Senthil K., Uppoor G. Bhat, Douglas E. Hughes, I-Ching Wang, Robert H. Costa, and Andrei L. Gartel. 2006. “Identification of a Chemical Inhibitor of the Oncogenic Transcription Factor Forkhead Box M1.” *Cancer Research* 66 (19): 9731–35.

Ramakrishna, Sneha, Il-Man Kim, Vladimir Petrovic, Dmitriy Malin, I.-Ching Wang, Tanya V. Kalin, Lucille Meliton, et al. 2007. “Myocardium Defects and Ventricular Hypoplasia in Mice Homozygous Null for the Forkhead Box M1 Transcription Factor.” *Developmental Dynamics* 236 (4): 1000–1013.

Raychaudhuri, P., and H. J. Park. 2011. “FoxM1: A Master Regulator of Tumor Metastasis.” *Cancer Research* 71 (13): 4329–33.

Russell, Paul, and Paul Nurse. 1986. “Cdc25+ Functions as an Inducer in the Mitotic Control of Fission Yeast.” *Cell* 45 (1): 145–53.

Sanchez, Yolanda, Calvin Wong, Richard S. Thoma, Ron Richman, Zhiqi Wu, Helen Piwnica-Worms, and Stephen J. Elledge. 1997. “Conservation of the Chk1 Checkpoint Pathway in Mammals: Linkage of DNA Damage to Cdk Regulation Through Cdc25.” *Science* 277 (5331): 1497–1501.

Sanders, Deborah A., Michael V. Gormally, Giovanni Marsico, Dario Beraldi, David Tannahill, and Shankar Balasubramanian. 2015. “FOXM1 Binds Directly to Non-Consensus Sequences in the Human Genome.” *Genome Biology* 16 (1): 130.

Shi, Y, P E Kroeger, and R I Morimoto. 1995. “The Carboxyl-Terminal Transactivation Domain of Heat Shock Factor 1 Is Negatively Regulated and Stress Responsive.” *Molecular and Cellular Biology* 15 (8): 4309–18.

Spengler, Mary L., and Michael G. Brattain. 2006. “Sumoylation Inhibits Cleavage of Sp1 N-Terminal Negative Regulatory Domain and Inhibits Sp1-Dependent Transcription.” *Journal of Biological Chemistry* 281 (9): 5567–74.

Swaffer, Matthew P., Andrew W. Jones, Helen R. Flynn, Ambrosius P. Snijders, and Paul Nurse. 2016. “CDK Substrate Phosphorylation and Ordering the Cell Cycle.” *Cell* 167 (7): 1750-1761.e16.

Toyoshima, Fumiko, Tetsuo Moriguchi, Atsushi Wada, Makoto Fukuda, and Eisuke Nishida. 1998. “Nuclear Export of Cyclin B1 and Its Possible Role in the DNA Damage-induced G2 Checkpoint.” *The EMBO Journal* 17 (10): 2728–35.

Ustiyan, Vladimir, I-Ching Wang, Xiaomeng Ren, Yufang Zhang, Jonathan Snyder, Yan Xu, Susan E. Wert, James L. Lessard, Tanya V. Kalin, and Vladimir V. Kalinichenko. 2009. “Forkhead Box M1 Transcriptional Factor Is Required for Smooth Muscle Cells during Embryonic Development of Blood Vessels and Esophagus.” *Developmental Biology* 336 (2): 266–79.

Wang, F., C. B. Marshall, K. Yamamoto, G.-Y. Li, G. M. C. Gasmi-Seabrook, H. Okada, T. W. Mak, and M. Ikura. 2012. “Structures of KIX Domain of CBP in Complex with Two FOXO3a Transactivation Domains Reveal Promiscuity and Plasticity in Coactivator Recruitment.” *Proceedings of the National Academy of Sciences* 109 (16): 6078–83.

Wang, I.-Ching, Yi-Ju Chen, Douglas Hughes, Vladimir Petrovic, Michael L. Major, Hyung Jung Park, Yongjun Tan, Timothy Ackerson, and Robert H. Costa. 2005. “Forkhead Box M1 Regulates the Transcriptional Network of Genes Essential for Mitotic Progression and Genes Encoding the SCF (Skp2-Cks1) Ubiquitin Ligase.” *Molecular and Cellular Biology* 25 (24): 10875–94.

Wang, Zebin, Hyun Jung Park, Janai R. Carr, Yi-ju Chen, Yu Zheng, Jing Li, Angela L. Tyner, Robert H. Costa, Srilata Bagchi, and Pradip Raychaudhuri. 2011. “FoxM1 in Tumorigenicity of the Neuroblastoma Cells and Renewal of the Neural Progenitors.” *Cancer Research* 71 (12): 4292–4302.

Wierstra, Inken, and Jürgen Alves. 2006. “Despite Its Strong Transactivation Domain, Transcription Factor FOXM1c Is Kept Almost Inactive by Two Different Inhibitory Domains.” *Biological Chemistry* 387 (7): 963–76.

Wonsey, Diane R., and Maximillian T. Follettie. 2005. “Loss of the Forkhead Transcription Factor FoxM1 Causes Centrosome Amplification and Mitotic Catastrophe.” *Cancer Research* 65 (12): 5181–89.

Wright, Peter E., and H. Jane Dyson. 2015. “Intrinsically Disordered Proteins in Cellular Signalling and Regulation.” *Nature Reviews Molecular Cell Biology* 16 (1): 18–29.

Xu, Haiyan, Chelsea L. Gustafson, Patrick J. Sammons, Sanjoy K. Khan, Nicole C. Parsley, Chidambaram Ramanathan, Hsiau-Wei Lee, Andrew C. Liu, and Carrie L. Partch. 2015. “Cryptochrome 1 Regulates the Circadian Clock through Dynamic Interactions with the BMAL1 C Terminus.” *Nature Structural & Molecular Biology* 22 (6): 476–84.

Chapter 2: Phosphorylation of FoxM1 dictates association with regulatory partners

2.1. Introduction

Phosphorylation is a conserved mechanism of protein regulation and plays critical roles in timing and execution of the mitotic program (Swaffer et al. 2016; Barik et al. 2010; Alberts et al. 2002; Rhind and Russell 2012). The majority of data and hypotheses in the field of FoxM1 regulation indicate that Cdks are the primary driver of FoxM1 activation (Anders et al. 2011; Major, Lepe, and Costa 2004; J. Laoukili et al. 2008; Lüscher-Firzlaff, Lilischkis, and Lüscher 2006). While it is evident that Cdks play a crucial role in FoxM1 activation, understanding the mechanism by which Cdks activate FoxM1 is not explicitly known. FoxM1 undergoes phosphorylation by Cdks beginning in the G1/S transition as we begin to see FoxM1 expression rise. As the cell cycle progresses, we see increasing levels of Cdk phosphorylated FoxM1 protein levels as well as FoxM1 transcriptional activity. Consequently, the role of Cdk is known to be critical for FoxM1 activity (Swaffer et al. 2016; Major, Lepe, and Costa 2004).

In addition to the role of Cdks in FoxM1 activation, there is an increasing amount of data indicating that Plk1 may have a direct role in FoxM1 activity. As the cell cycle progresses across the G2/M transition we see increasing levels of FoxM1 phosphorylation by Plk1 (Fu et al. 2008). We also know that Plk1 is a bona fide FoxM1 target gene and the subsequent expression of Plk1 leads to the establishment of a positive feedback loop whereby Plk1 expression leads to increased FoxM1 activity (Jamila Laoukili et al. 2005; Fu et al. 2008). Plk1 has a conserved mechanism of phosphorylation that requires binding to Cdk phosphorylated residues and subsequent phosphorylation. Plk1 contains tandem polobox domain that bind to Cdk phosphorylated residues at polobox binding substrate sites that allow subsequent phosphorylation of an N-terminal kinase domain (Lee et al. 2014, 1). Subsequently, the coordination of Cdks and Plk1 activity likely plays a crucial role in the overall activation of FoxM1 throughout the cell cycle. This dissertation describes the detailed

mechanism by which both Cdks and Plk1 activate FoxM1 and coordinately drive transcriptional activation across the G2/M transition.

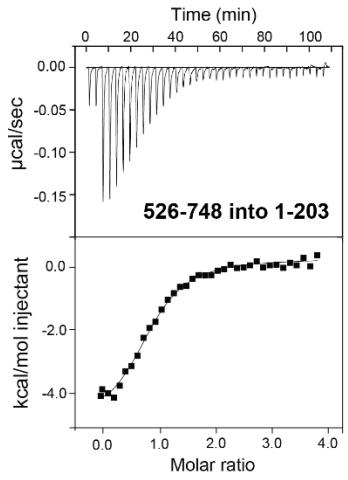
2.2. Results

2.2.1. FoxM1 NRD directly binds the TAD

Performed by co-author of this study Dr. Aimee Marceau

To assess the model that FoxM1 NRD inhibits transcription by sequestration of the TAD we tested binding of FoxM1 domains *in vitro*. The FoxM1 NRD inhibits transcription factor transactivation activity early in the cell cycle. Transcription reporter assays suggest that the NRD negatively regulates the TAD through a sequestration mechanism (Park et al., 2008b; Wierstra and Alves, 2006a). To confirm a direct interdomain association and to define more precisely the NRD and TAD domain boundaries, we purified recombinant protein constructs of various lengths and assayed their association *in trans* using isothermal titration calorimetry (ITC) (Figure 1.2). We first used an NRD-containing construct that includes the entire N-terminus of FoxM1 up until near the start of the DBD (residues 1-203 in human isoform FoxM1b) and a long C-terminal construct (residues 526-748) including the Cdk-site rich region (CSR) and putative TAD. We observe binding between these protein fragments and measured an affinity of K_d = 2 ± 1 μM (Figure 1B and 1C). Using sequence conservation we designed a minimal NRD (1-114) and minimal TAD (696-748) and found that they associate with comparable affinity (K_d = 3 ± 2 μM). When we attempted to shorten the constructs further, we found loss of affinity (Figure 2.1), so we conclude that these fragments contain the approximate sequences necessary and sufficient for interdomain association.

A



B

N-term	C-term	K_d(µM)
1-203	526-748	2 ± 1
1-114	696-748	3 ± 2
1-16	696-748	no heat
80-114	696-748	no heat
1-203	694-726	> 10
1-203	727-748	no heat
1-117/ 694-748	696-748	no heat

Figure 2.1: FoxM1 NRD directly binds TAD *in vitro*. (A) Isothermal titration calorimetry (ITC) data indicate association between purified TAD and NRD-containing constructs. **(B)** ITC affinity measurements for the indicated purified protein constructs. Domains are indicated as in **Figure 1.2**.

2.2.2. FoxM1 directly binds to co-activator CBP

The requirement of Cdk phosphorylation for FoxM1 activity has been linked to FoxM1 recruitment of the co-activator acetyltransferase proteins CBP and p300 (Major et al., 2004). These co-activators share high sequence homology and contain several protein-protein interaction domains that associate with transcription factor TADs (Wang et al., 2013). We tested three common TAD interaction domains in CBP and found that purified TAZ2 and KIX domains bind the FoxM1 TAD, while TAZ1 does not. The TAZ2 and KIX domains bind with 0.7 ± 0.3 and 2.7 ± 0.5 µM affinity, respectively (Figure 2.2A). For future structural studies and binding assays, we focus on TAZ2 binding to TAD due to the higher affinity.

2.2.3. FoxM1 TAD cannot simultaneously bind multiple domains of CBP

Previous literature has indicated that forkhead box protein TADs can contain multiple distinct binding regions within the functional TAD, and that these regions can bind discrete regions of CBP domains (Wang et al. 2012). This raises questions regarding a potential for

bimodal binding capacity of the TAD. More specifically, we aim to test the binding of the FoxM1 TAD – as defined in this study – and it's potential to be truncated into sub-domains that bind CBP. Additionally, we aim to test the TADs ability or lack thereof to bind to multiple domains of CBP simultaneously.

We designed small TAD fragments based on conservation and assayed the ability of the fragments to bind to TAZ2. We see that neither the N-terminal fragment (694-726) nor the C-terminal fragment (727-748) can bind CBP-TAZ2, indicating that the FoxM1 TAD as defined in this study is the minimal functional TAD. In addition, when we competitively titrate CBP fragments into bound CBP-TAD complexes we see binding in a manner that seems to be dictated purely by affinity. To test the competitive binding for the TAD, we use ITC to assay for competition between CBP domains for TAD. Upon titration of TAD with KIX we see a binding affinity of approximately 3 μM. Subsequent titration of TAZ2 gives heats by ITC and an apparent K_d of approximately 2 μM. However, if we first saturate TAD with TAZ2 and assay for binding of KIX to TAD:TAZ2 complex we see no heats by ITC. This indicates that rather than a mechanism of bimodal binding, FoxM1 binds either KIX or TAZ2 in a manner dependent of affinity and cellular availability (Figure 2.2C).

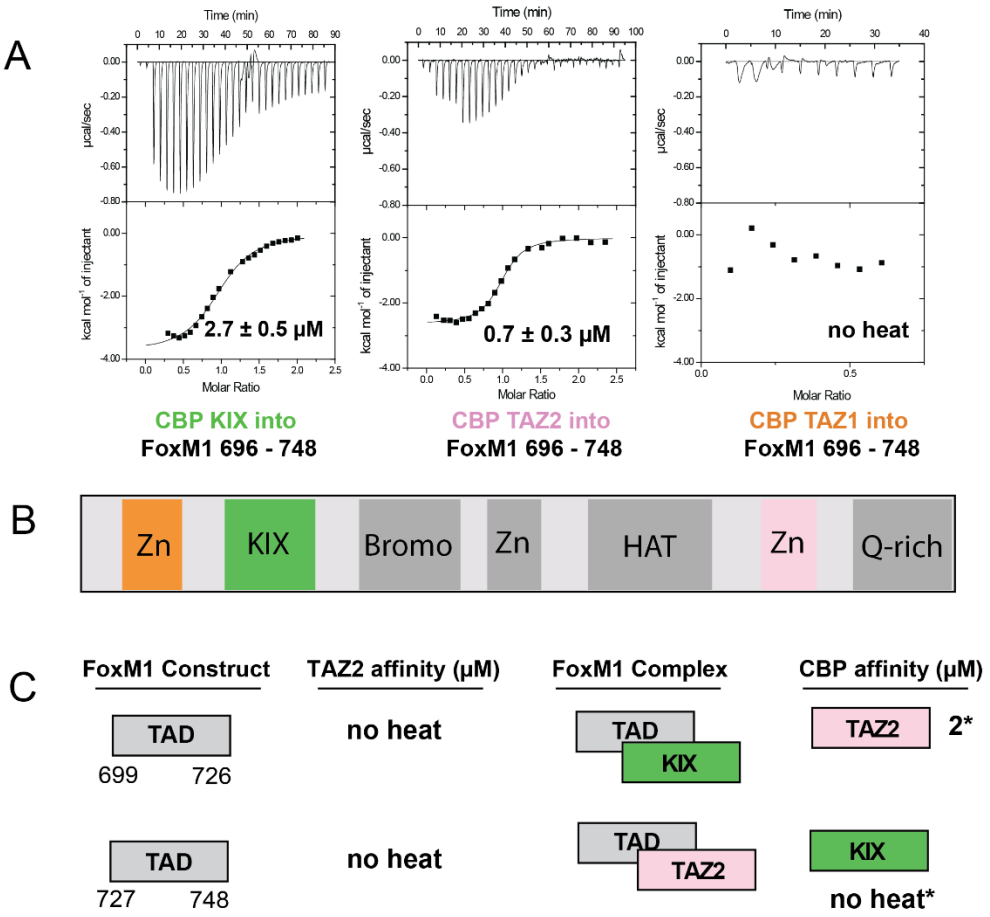


Figure 2.2: FoxM1 binds CBP. (A) Raw ITC data and the calculated affinities of FoxM1 TAD (696-748) binding to the KIX, TAZ1, and TAZ2 domains of CBP. **(B)** CBP domain architecture highlighting the domains of interest; TAZ2 (pink), KIX (green), and TAZ1 (orange). **(C)** ITC affinities of the indicated FoxM1 construct for TAZ2 and CBP fragments in competition. *n = 1.

2.2.4 CBP cannot bind auto-repressed FoxM1

We could not detect binding of the NRD-TAD fusion protein to the TAZ2 domain using ITC, and we observed weak association to an NRD-TAD complex using NMR (Figure 2.3). The fusion protein containing the I88A interface mutation did bind in the ITC assay, albeit with slightly weaker affinity than the TAD alone (Figure 2.3A). These results support the model that the NRD inhibits FoxM1 activity by sequestering the TAD from interacting with transcriptional co-activators.

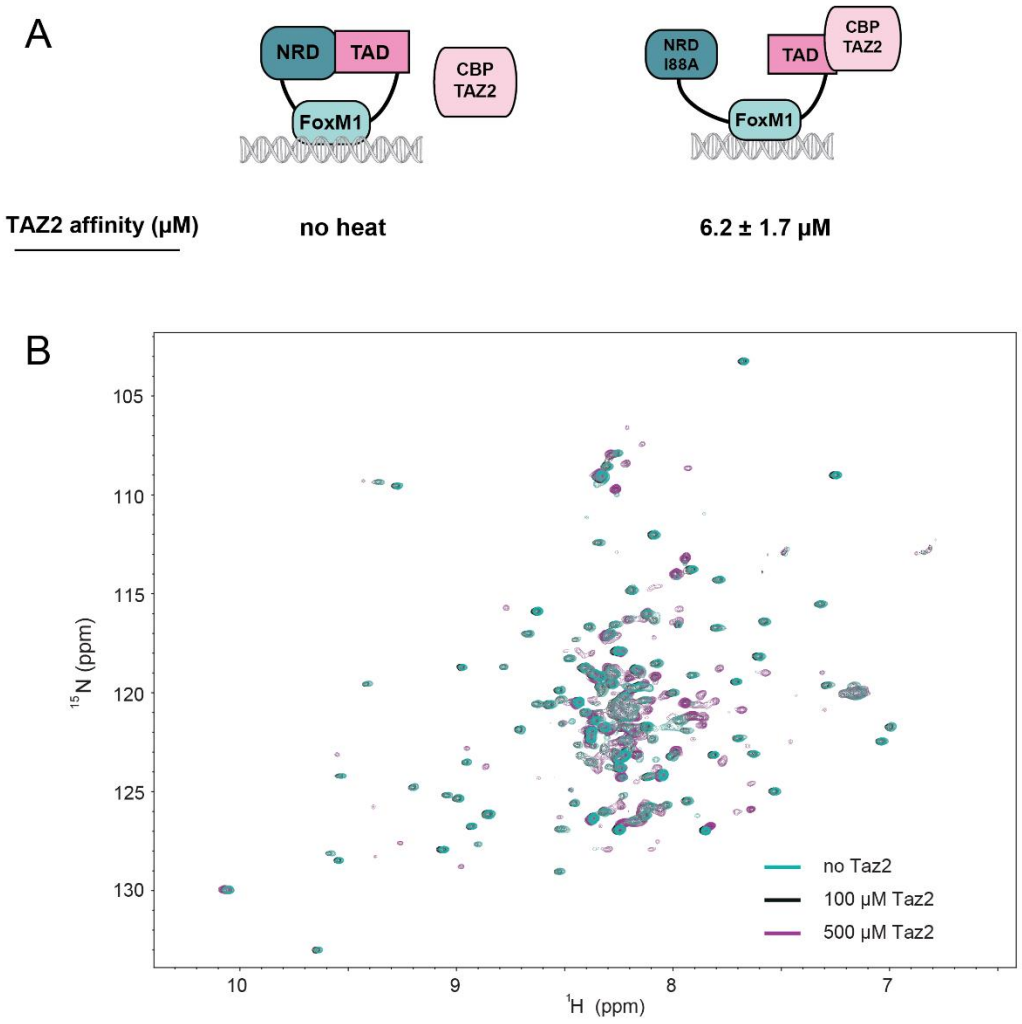


Figure 2.3: CBP cannot bind auto-repressed FoxM1. (A) Affinities of WT and I88A NRD-TAD fusion for TAZ2. **(B)** NMR HSQC of 100 μM FoxM1 NRD-TAD fusion with excess TAZ2 titrated in. Titration concentrations are indicated, 1 M equivalent and 5 M excess, respectively.

2.2.5. Cdk phosphorylation has no direct effect on NRD-TAD binding

Performed by co-author of this study Dr. Aimee Marceau

In the current accepted model, Cdk phosphorylation relieves NRD inhibition by directly destabilizing the NRD-TAD association (Anders et al., 2011; Laoukili et al., 2008a; Park et al., 2008b; Wierstra and Alves, 2006b). We addressed with purified domains whether phosphorylation of Cdk sites in human FoxM1 directly affects the inhibitory NRD-TAD association. For these assays, we phosphorylated Cdk consensus sites using Cdk2-Cyclin A (Cdk2-CycA) as previously described (McGrath et al., 2017), we verified phosphorylation by electrospray mass spectrometry, and we measured affinities using the ITC assay. We first observed that phosphorylation of the NRD, which contains a single conserved consensus Cdk site (S4), has minimal effect on the affinity of the NRD for the CSR-TAD. While there are no consensus Cdk sites in the TAD, there are several sites in the Cdk site region (CSR). To test if Cdk phosphorylation of this region directly affects the NRD-TAD association, we generated protein constructs in which the CSR is included with the TAD or fused to the NRD. The CSR-TAD construct (amino acids 526-748) binds the NRD with similar affinity whether or not it is first phosphorylated with Cdk2-CycA (Figure 4A). The NRD-CSR fusion protein (amino acids 1-114 + 526-674) binds the TAD with similar affinity as the NRD alone and with similar affinity whether or not it is first phosphorylated with Cdk2-CycA. These measurements are consistent with the lack of Cdk sites near the NRD-TAD interface in our structural model. The observation here that phosphorylation of Cdk consensus sites has no direct effect on the repressive NRD-TAD interaction suggests that Cdk phosphorylation is not sufficient for activation of the FoxM1 transcription factor (2.4A).

2.2.6. Cdk phosphorylation has no effect on CBP binding to FoxM1

Performed by co-author of this study Dr. Aimee Marceau

Cdk phosphorylation has long been assumed to be the primary driver of FoxM1 activation (Major, Lepe, and Costa 2004; J. Laoukili et al. 2008; Lüscher-Firzlaff, Lilischkis,

and Lüscher 2006). Under the belief that FoxM1 activation is Cdk phosphorylation dependent you would expect that Cdk phosphorylation would play a role in changing the affinity between FoxM1 TAD and co activator CBP. We see no change in affinity upon Cdk phosphorylation between FoxM1 TAD-CSR and CBP TAZ2. Regardless of phosphorylation state we see an affinity of approximately 1.5 µM between CBP TAZ2 and FoxM1 TAD-CSR thus showing that Cdk phosphorylation plays no role in direct enhancement of association with co-activator (Figure 2.4B).

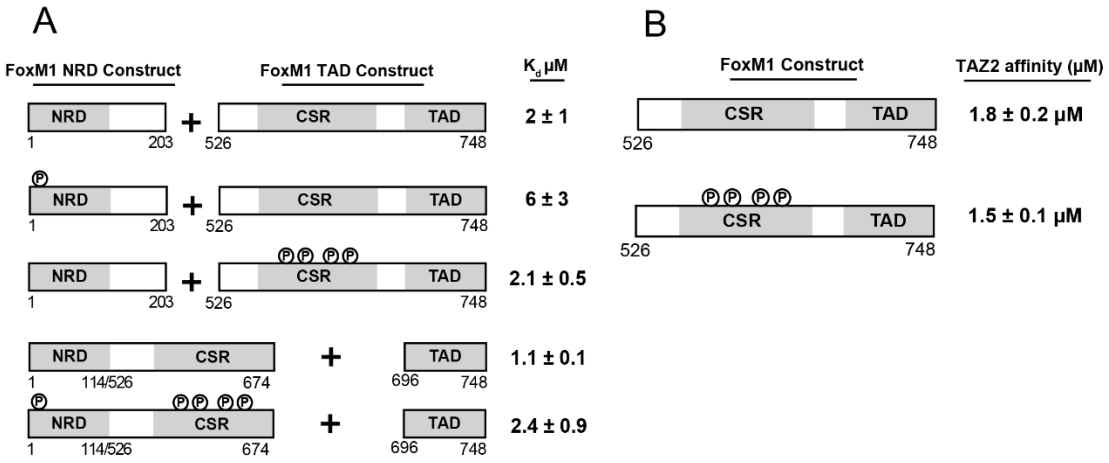


Figure 2.4: Cdk phosphorylation has no direct role in regulation of FoxM1 interactions. **(A)** Purified and isolated domains of FoxM1 were titrated and affinities were determined by ITC. Phosphorylation states are indicated in the CSR and/or NRD. **(B)** Purified and isolated domains of CBP were assayed for binding to FoxM1 CSR-TAD and affinities were determined by ITC. Cdk phosphorylation sites are indicated in the CSR.

2.2.7. Plk phosphorylation has no effect on CBP binding to FoxM1

In similar vain to Cdk phosphorylation of FoxM1, Plk1 activity has been shown to enhance transcriptional activity of FoxM1 in a dose dependent manner (Fu et al. 2008). Under the belief that FoxM1 activation is enhanced by Plk1 activity, you could expect Plk1 phosphorylation of the FoxM1 TAD to enhance the binding to co-activator CBP. To test this, we phosphorylated the FoxM1 TAD by incubating with purified Plk1, and we confirmed quantitative phosphorylation of 4 sites (Ser702, Ser715, Ser724, and Ser741) with electrospray mass spectrometry. Upon phosphorylation of either the FoxM1 CSR-TAD or

TAD alone by Plk1 *in vitro* we see no significant change in affinity between a phosphorylated and unphosphorylated state (Plk1 data not shown).

2.2.8. Plk1 phosphorylation obliterates NRD binding

Performed by co-author of this study Dr. Aimee Marceau

Plk1 activity has also been implicated in FoxM1 activation (Fu et al., 2008). The FoxM1 TAD contains 5 potential serine Plk1 phosphorylation sites. We phosphorylated the FoxM1 TAD by incubating with purified Plk1, and we confirmed quantitative phosphorylation of 4 sites (Ser702, Ser715, Ser724, and Ser741) with electrospray mass spectrometry. These sites are all conserved (Figure 1.2), and two of them (Ser715 and Ser724) were previously identified as Plk1 sites in cells (Fu et al., 2008). We observed that the Plk1 phosphorylated-TAD no longer binds the NRD by ITC (Figure 2.5). Using TAD constructs with serine to alanine mutations, which cannot be phosphorylated, we tested the importance of specifically phosphorylating Ser715 on the NRD-TAD affinity. When the three other Plk1 sites are mutated, the phosphorylated TAD still lacks any detectable affinity for the NRD. In contrast, phosphorylation of a Ser715A construct results in no change in affinity. We conclude that Ser715 phosphorylation by Plk1 is necessary and sufficient for inhibiting the NRD-TAD association. In addition, we see when U2OS cells are transfected with a TAD mutant that cannot be phosphorylated by Plk1 at site 715 (S715A) we see no enhancement of transcriptional activity. This contrasts with I88A NRD mutation which destabilizes the NRD-TAD association in which we see enhancement of transcriptional activity. We see no significant change in transcriptional activation upon TAD mutant V708A/L709A that disrupts the NRD-TAD association likely to a disruption of co-activator recruitment. We test this hypothesis in **Chapter 3**. This indicates that the phosphorylation event is linked to de-repression and when TAD cannot be phosphorylated at 715 the TAD cannot be de-repressed. These results are consistent with and explain the previous report that an

Ser715A/Ser724A mutation decreases FoxM1 activation of several mitotic genes in U2OS cells (Fu et al., 2008).

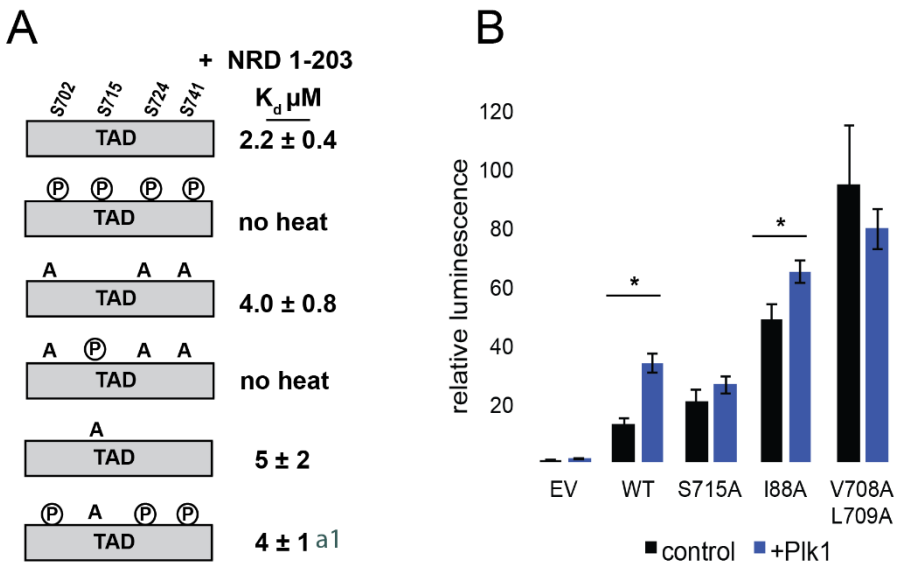


Figure 2.5: Phosphorylation of the TAD by Plk1 regulates NRD-TAD interactions. (A) ITC binding affinity of NRD 1-203 for WT TAD and TAD containing mutations at Plk1 sites. Measurements were made with and without Plk1 phosphorylation. **(B)** Luciferase reporter expression from the 6DB promoter. Only experiments in which significant differences in the relative luminescence between expression of FoxM1 alone (control, black) or co-expression with Plk1 (purple) are indicated with asterisks (* $p < 0.05$, using two-tailed student's t-test).

2.2.9. Cdk phosphorylation of the CSR allows Plk1 polobox binding domain association

Performed by co-author of this study Dr. Aimee Marceau

Plk1 has tandem polobox binding domains that allow Plk1 to bind to phosphorylated Cdk substrates and allow for subsequent phosphorylation with an N-terminal kinase domain (Lee et al. 2014). This mechanism is conserved among the Polo-like kinase family from yeast to humans. FoxM1 has a polobox binding domain in the CSR, specifically residue 585. To test for an association between Plk1 polobox binding domain and CSR we purified isolated domains and tested for their binding by ITC. We see that unphosphorylated CSR does not bind the polobox domain of Plk1. Conversely, the Cdk phosphorylated CSR binds the polobox domain of Plk1 with nanomolar affinity (Figure 2.6).

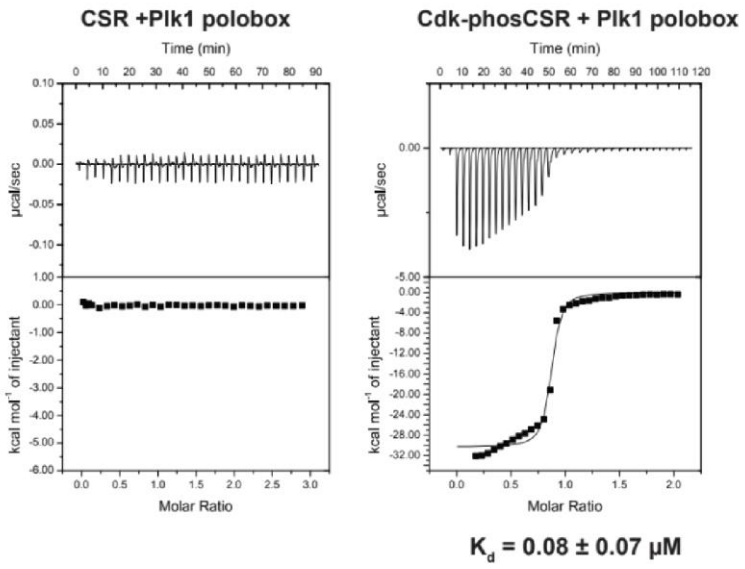


Figure 2.6: Plk1 polobox binding domain binds Cdk phosphorylated CSR. Isolated and purified domains were assayed for binding by ITC. Affinities are reported below. No heat by ITC is no reported affinity.

2.2.10. Conclusions

. This study details the narrative of FoxM1 activation through the lens of de-repression of the NRD in a phosphorylation dependent manner. This study concludes that Cdk phosphorylation plays no direct role in relief of repression from the NRD, but rather that phosphorylation of the CSR by Cdk allows for Plk1 to bind and phosphorylate the C-terminal TAD. The phosphorylation of the TAD, specifically at S715, disallows sequestration of the TAD by the NRD and maintains binding capacity to transcriptional co-activator CBP.

2.3. Discussion

The idea that different phosphorylation events have specific and distinct roles is in contrast to several proposed models for multisite phosphorylation in the cell cycle, in which a threshold aggregate of redundant phosphorylation events drives a change in protein activity (Harvey et al., 2005; Kim and Ferrell, 2007; Nash et al., 2001). Our observation of specificity in the effects of FoxM1 phosphorylation more resembles what has been proposed for the retinoblastoma protein, in which specific phosphorylation events drive distinct structural changes or protein-protein interactions (Rubin, 2013). While Cdks and Plk1 have been or are cancer therapeutic targets, this can provide more insight into targeting the FoxM1 pathway for cancer. This work clarifies the role of Cdks and Plk1 and can help guide more targeted cancer kinase therapeutics acting upstream of FoxM1.

2.4. Materials and Methods

Protein Expression

The human FoxM1 constructs (1-114, 1-203, 1-332, 80-114, 1-117/694-748 fusion, 1-117/694-748 fusion Δ25-50, 1-114/526-674 fusion, 573-635, 526-748, and 696-748) were expressed in and purified from *E. coli* as N-terminal GST fusion proteins with TEV cleavage sites. Cells were induced in mid-log phase with 1 mM IPTG, cells were grown for 3-4 hours at 25 °C. All proteins were purified from lysates with glutathione sepharose affinity chromatography. Fusion and C-terminal (TAD) constructs were further purified with Q-sepharose and then cleaved with TEV protease. Proteins were buffer exchanged into 25 mM Tris, 1 M NaCl, 5 mM DTT (pH 8.0) and then passed over glutathione sepharose resin to remove free GST, concentrated, and run over Superdex-75 (GE Healthcare) into 20 mM HEPES pH 7.5, 150 mM NaCl, 5% glycerol. After TEV cleavage, N-terminal (NRD) constructs were diluted in 20 mM Hepes, 5 mM DTT (pH 7.0), and purified with S-sepharose and Superdex-75 as described for C-terminal constructs.

Human Plk1 kinase domain (13-345) was expressed with an N-terminal His tag in Sf9 cells using the FastBac expression system. Cells were harvested and lysed in a buffer containing 50 mM Tris, 300 mM KCl, 2 mM $MgCl_2$, 10 mM Imidazole (pH 8.0), Sigma Protease Inhibitor (P8340) and 2mM phenylmethylsulfonyl fluoride. Protein was purified with Nickel Sepharose Excel resin (GE Healthcare) equilibrated in lysis buffer. The resin was washed with a buffer containing 1 M KCl, 50 mM Tris, 40 mM Imidazole, 10 mM BME, 2 mM $MgCl_2$ (pH 8.0) and protein was eluted in 200 mM KCl, 50 mM Tris, 300 mM Imidazole, 10 % glycerol v/v, 10 mM BME, 2 mM $MgCl_2$ (pH 8.0). Protein was dialyzed into storage buffer (200 mM KCl, 50 mM Tris 8, 10 mM BME, 2 mM $MgCl_2$, 10% glycerol v/v, (pH 8.0)) and stored at -80˚C. The polobox domain of human Plk1 and Cdk2-CycA were expressed and purified as previously described (Cheng et al., 2003; McGrath et al., 2013).

Mus musculus CBP KIX (CBP residues 567-653), TAZ2 (residues 1764-1855) and TAZ1 (residues 340-439) were expressed in *E. coli*. KIX was expressed with a His tag and first purified using nickel sepharose affinity chromatography as described above. TAZ2 was expressed as an MBP fusion protein and purified using amylose sepharose affinity chromatography and S-sepharose ion exchange chromatography. The TAZ2 contained cysteine to alanine point mutations (C1776A, C1784A, C1827A, C1828A) that increase solubility and stability (De Guzman et al., 2000). $ZnSO_4$ was kept in growth media for TAZ2 growth at a concentration of 1 µM. TAZ1 was expressed with a His-Nus-XL affinity tag and purified using nickel affinity resin followed by tag cleavage. All CBP domains were further purified with Superdex 75 size exclusion chromatography.

Isothermal titration calorimetry

Equilibrium dissociation constants for FoxM1 NRD constructs binding to TAD constructs were obtained using ITC with a MicroCal VP-ITC system. FoxM1 protein

fragments were run over Superdex-75 (GE Healthcare) into 20 mM HEPES pH 7.5, 150 mM NaCl, 5% glycerol. TAD fragments (100-500 µM) were titrated into the NRD fragments (10-50 µM) at 25°C. The equilibrium dissociation constant for FoxM1 CSR binding to the Plk1 polobox domain was similarly determined. CSR (300 µM), either phosphorylated or unphosphorylated with Cdk2-CycA, was titrated into polobox (30 µM) at 25°C. Reported K_d values are the average fits from two or three technical replicates with the standard deviation reported as error. For data fitting in experiments involving the FoxM1 NRD, we adjusted NRD concentration such that the stoichiometry was close to 1. We chose this approach for the fitting, because we otherwise noticed variability in the n value that we attribute to difficulty measuring the NRD concentration from its low extinction coefficient. If no significant heat was detected above background, we conclude no association. In the case of titrating the TAD fragment 694-726 into 1-203, we observed small heats but could not fit the data, so we conclude the affinity must be weaker than 10 µM.

Equilibrium dissociation constants for CBP domain binding to FoxM1 TAD were obtained using ITC with Micro Cal VP-ITC system. Both FoxM1 and CBP proteins were run over Superdex-75 (GE Healthcare) into 20 mM HEPES 7.5, 150 mM NaCl, 5% glycerol v/v. CBP-TAZ2 (250-350 µM) was titrated into FoxM1 TAD (20 – 40 µM) at 25ºC. Because of the difficulty in determining CBP-TAZ2 concentrations, the concentrations were adjusted to a stoichiometry of 1.0. CBP-KIX (600 µM) was titrated into FoxM1 TAD (60 µM) at 30˚C in the same buffer. Reported K_d values are the average fits from two or three technical replicates with the standard deviation reported as error.

Kinase reactions

FoxM1 protein constructs following final purification were incubated with 10 mM ATP, 50 mM $MgCl_2$, and 10% by mass of either Plk1 kinase domain, Cdk2-CycA, or both Plk1 and Cdk2-CycA, overnight at 4 °C. Phosphorylation of the protein was confirmed by electrospray mass spectrometry using a Sciex X500B QTOF system.

Cell culture

Human osteosarcoma U2OS cells were maintained in Dulbecco's modified Eagle's medium (DMEM) containing 10% fetal bovine serum, 2mM L-glutamine, and 1x Penicillin Streptomycin and split every 2-3 days. Cells tested negative for Mycoplasma contamination using a PCR assay.

Reporter assays were performed using the FoxM1c isoform, which includes 15 amino acids downstream of the DNA binding domain that are absent in FoxM1b. The amino acid sequence of the NRD, CSR and TAD domains are identical in FoxM1c and FoxM1b. For clarity, mutations are indicated using FoxM1b numbering throughout the figures and text. Mutants were expressed from the pCDNA3 plasmid with and contain an N-terminal FLAG tag: pCDNA3-FOXM1C (WT), pCDNA3-FOXM1C-I88A, pCDNA3-FOXM1C-S715A, pCDNA3-FOXM1C-V708A, L709A. The day prior to transient transfections, $2x10^5$ U2OS cells were seeded into 12-well plates in antibiotic-free medium (DMEM/ 10%FBS/L-glutamine). Cells were then transfected with Lipofectamine 2000 Reagent (Invitrogen 11668-019) according to the manufacturer's protocol with 650ng pGL3-6DB-reporter. Cell lysates were prepared 25 hours post-transfection using the Promega Dual Luciferase Reporter Assay System kit (Promega, E1960) and luminescence was measured on a Promega Glo Max. Relative luminescence was determined by normalizing the Firefly luciferase activity (expressed by pGL3 reporter plasmids) activity to Renilla Luciferase (transfection efficiency control). Three technical replicate transfections were performed in each experiment and each experiment was carried out three times (biological replicates). Analysis was performed in Excel and GraphPad Prism software.

NMR Sample prep

NMR experiments for resonance assignment were performed on a Bruker Avance III HD 800-MHz spectrometer equipped with a cryogenically cooled probe head. All samples were prepared in a buffer containing 20 mM sodium phosphate pH 6.3, 100 mM KCl, and 5%

(v/v) D_2O. Dr FoxM1 NRD-TAD apo spectra was acquired at 100 µM and 1 M equivalent unlabeled CBP-TAZ2 was titrated in. In a separate NMR tube, 100 µM Dr FoxM1 NRD-TAD and 5 M excess CBP-TAZ2 spectra was acquired to compensate for changes in volume upon titration. Data was processed with NMRPipe and analyzed with CCPNmr (Vranken et al. 2005; Delaglio et al. 1995).

2.5 References

Alberts, Bruce, Alexander Johnson, Julian Lewis, Martin Raff, Keith Roberts, and Peter Walter. 2002. “Components of the Cell-Cycle Control System.” *Molecular Biology of the Cell. 4th Edition*.

Anders, Lars, Nan Ke, Per Hydbring, Yoon J. Choi, Hans R. Widlund, Joel M. Chick, Huili Zhai, et al. 2011. “A Systematic Screen for CDK4/6 Substrates Links FOXM1 Phosphorylation to Senescence Suppression in Cancer Cells.” *Cancer Cell* 20 (5): 620–34.

Barik, Debashis, William T Baumann, Mark R Paul, Bela Novak, and John J Tyson. 2010. “A Model of Yeast Cell-Cycle Regulation Based on Multisite Phosphorylation.” *Molecular Systems Biology* 6 (August).

Delaglio, F., S. Grzesiek, G. W. Vuister, G. Zhu, J. Pfeifer, and A. Bax. 1995. “NMRPipe: A Multidimensional Spectral Processing System Based on UNIX Pipes.” *Journal of Biomolecular NMR* 6 (3): 277–93.

Fu, Zheng, Liviu Malureanu, Jun Huang, Wei Wang, Hao Li, Jan M. van Deursen, Donald J. Tindall, and Junjie Chen. 2008. “Plk1-Dependent Phosphorylation of FoxM1 Regulates a Transcriptional Programme Required for Mitotic Progression.” *Nature Cell Biology* 10 (9): 1076–82.

Joshi, Kaushal, Yeshavanth Banasavadi-Siddegowda, Xiaokui Mo, Sung-Hak Kim, Ping Mao, Cenk Kig, Diana Nardini, et al. 2013. “MELK-Dependent FOXM1 Phosphorylation Is Essential for Proliferation of Glioma Stem Cells.” *Stem Cells (Dayton, Ohio)* 31 (6): 1051–63.

Laoukili, J., M. Alvarez, L. A. T. Meijer, M. Stahl, S. Mohammed, L. Kleij, A. J. R. Heck, and R. H. Medema. 2008. “Activation of FoxM1 during G2 Requires Cyclin A/Cdk-Dependent Relief of Autorepression by the FoxM1 N-Terminal Domain.” *Molecular and Cellular Biology* 28 (9):

Laoukili, Jamila, Matthijs R. H. Kooistra, Alexandra Brás, Jos Kauw, Ron M. Kerkhoven, Ashby Morrison, Hans Clevers, and René H. Medema. 2005. “FoxM1 Is Required for Execution of the Mitotic Programme and Chromosome Stability.” *Nature Cell Biology* 7 (2): 126–36.

Lee, Kyung S., Jung-Eun Park, Young Hwi Kang, Tae-Sung Kim, and and Jeong K. Bang. 2014. “Mechanisms Underlying Plk1 Polo-Box Domain-Mediated Biological Processes and Their Physiological Significance” 37 (4): 286–94.

Lüscher-Firzlaff, Juliane M., Richard Lilischkis, and Bernhard Lüscher. 2006. “Regulation of the Transcription Factor FOXM1c by Cyclin E/CDK2.” *FEBS Letters* 580 (7): 1716–22.

Major, M. L., R. Lepe, and R. H. Costa. 2004. “Forkhead Box M1B Transcriptional Activity Requires Binding of Cdk-Cyclin Complexes for Phosphorylation-Dependent Recruitment of P300/CBP Coactivators.” *Molecular and Cellular Biology* 24 (7): 2649–61.

Rhind, Nicholas, and Paul Russell. 2012. “Signaling Pathways That Regulate Cell Division.” *Cold Spring Harbor Perspectives in Biology* 4 (10): a005942.

Rubin, Seth M. 2013. “Deciphering the Retinoblastoma Protein Phosphorylation Code.” *Trends in Biochemical Sciences* 38 (1): 12–19.

Swaffer, Matthew P., Andrew W. Jones, Helen R. Flynn, Ambrosius P. Snijders, and Paul Nurse. 2016. “CDK Substrate Phosphorylation and Ordering the Cell Cycle.” *Cell* 167 (7): 1750-1761.e16.

Vranken, Wim F., Wayne Boucher, Tim J. Stevens, Rasmus H. Fogh, Anne Pajon, Miguel Llinas, Eldon L. Ulrich, John L. Markley, John Ionides, and Ernest D. Laue. 2005. “The CCPN Data Model for NMR Spectroscopy: Development of a Software Pipeline.” *Proteins: Structure, Function, and Bioinformatics* 59 (4): 687–96.

Wang, F., C. B. Marshall, K. Yamamoto, G.-Y. Li, G. M. C. Gasmi-Seabrook, H. Okada, T. W. Mak, and M. Ikura. 2012. “Structures of KIX Domain of CBP in Complex with Two FOXO3a Transactivation Domains Reveal Promiscuity and Plasticity in Coactivator Recruitment.” *Proceedings of the National Academy of Sciences* 109 (16): 6078–83.

Chapter 3: FoxM1 structural confirmations and dynamics

3.1 Introduction

Structural plasticity and dynamics are a highly conserved mechanism of regulation across eukaryotic transcription factors (Minezaki et al. 2006; Liu et al. 2006; Bah et al. 2015). We understand that transcription factors will often fold into secondary structure upon binding to partners and we see this mechanism commonly among transcription factors that bind to CBP (F. Wang et al. 2012; Mujtaba et al. 2004; Goto et al. 2002). An excellent example of this regulation is the hormone receptor activator ACTR bound to CBP domain NCBD. Upon binding to CBP the ACTR gains α-helical structure from a disordered state. In addition, the NCBD transitions from a globule state with helical propensity to an α-helical structure (Ebert et al. 2008). We see this pattern of folding upon binding across many transcription factors and this work details the mechanism by which FoxM1 undergoes similar regulation.

While auto-regulatory repressive domains are common among transcription factors, there is very little mechanistic or structural insight on how auto-repression via transcription factors is regulated. This is likely due to the physical challenges of working with intrinsically disordered regions of transcription factors. Here we show through NMR and Rosetta modeling that the FoxM1 NRD-TAD auto-repressed complex forms a hydrophobic core. Alongside our structural model we highlight the importance of residues in that core for transcriptional regulation. Lastly, we show that FoxM1 undergoes distinct structural rearrangements dependent on binding association.

3.2. Results

3.2.1. The FoxM1 TAD has intrinsic disorder and partially globular domains

Performed in collaboration with co-author of this study Dr. Aimee Marceau

Outside of the winged helix DNA binding domain, FoxM1 is predicted to be primarily disordered outside highly conserved region of the TAD and NRD. While there has been a long-established belief that structure leads to function, the scientific community is beginning to understand the limits of structure and function. More specifically, the community of structural biologists is beginning to realize the importance of disorder in protein structure and function. The forkhead box family of proteins is predicted to be approximately 70% disordered as predicted by DISOPRED2 (Minezaki et al. 2006). Outside of the winged helix DNA binding domain, there remains no structural characterization of FoxM1 as a consequence (Littler et al. 2010). Sequence prediction software programs predict that FoxM1 could present small regions of structure within the NRD and the TAD, but due to the inherent plasticity of these domains no structures have been solved. FoxM1 is thusly characterized primarily as a transcription factor with high frequency of intrinsically disordered regions.

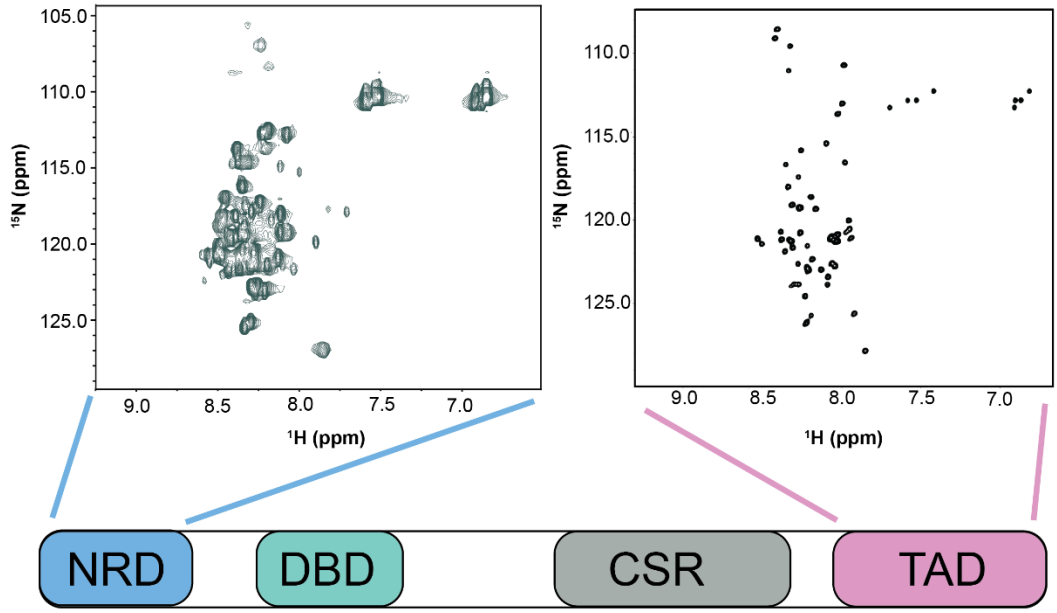


Figure 3.1: FoxM1 NRD and TAD are intrinsically disordered. NMR HSQC of both the apo NRD (left) and TAD (right) are shown above the domain architecture of full length human FoxM1. Both NRD and TAD show spectra with chemical shifts consolidated around 8.5 to 7.5 for amide proton, indicative of disorder.

3.2.2. FoxM1 NRD-TAD structural model

1. *Performed by co-author of this study Dr. Aimee Marceau in collaboration with Santrupti Nerli, Dr. Nikolaos Sgourakis, and Dr. Andrew McShan*

We combined NMR with Rosetta structural modeling to understand how the FoxM1 NRD binds the TAD in the autoinhibited conformation (Nerli and Sgourakis 2019). NMR studies of TAD-coactivator complexes have primarily utilized an approach in which the two domains are purified separately with isotope labeling of only one protein (De Guzman et al. 2006; I. Radhakrishnan et al. 1997; Zor et al. 2004). We found that spectra of the human NRD-TAD complex assembled from independently purified domains were generally of poor quality. We alternatively purified a protein construct for structural studies in which the minimal NRD and TAD were fused by a short cleavable linker (1-117/694-748). This fusion protein

does not bind additional TAD *in trans,* which suggests that the TAD and NRD are associated within the fusion.

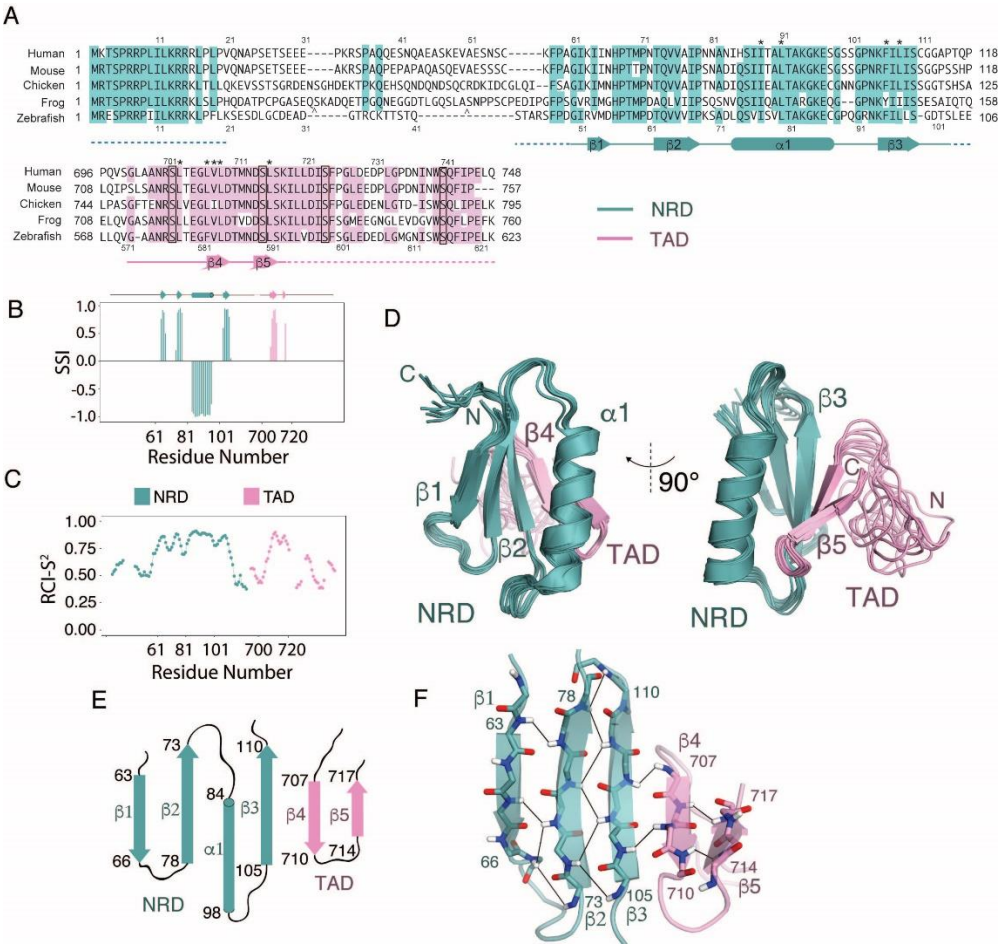


Figure 3.2: Solution structure of an NRD-TAD complex. (A) Sequence alignment of FoxM1 orthologs from *Homo sapiens* (human), *Mus musculus* (mouse), *Gallus gallus* (chicken), *Xenopus laevis* (frog), and *Danio rerio* (zebrafish). Conserved residues in at least four of the five sequences are colored. Secondary structure assignments are determined from dictionary of protein secondary structure (DSSP) analysis of the final NMR ensemble (Kabsch and Sander, 1983). Dashed lines indicate residues that are present in the NMR construct but are not included in the structure calculations and are significantly disordered according to the backbone chemical shifts. The asterisks (*) mark residues for which interdomain (NRD-TAD) NOEs have been unambiguously assigned. The carets (^) mark poorly conserved sequence insertions not shown in the frog sequence. Plk1 phosphorylation sites in the TAD are boxed. **(B)** Secondary Structure Index (SSI) derived from TALOS-N analysis of backbone chemical shifts corresponding to residues in the NRD (cyan) and TAD (pink) domains. Positive SSI values are consistent with β-strand and negative values are consistent with α-helical structure. Amino acid numbering corresponding to the human sequence is used. **(C)** Estimated backbone order parameters (Random Coil Index RCI-S^2) derived from the chemical shifts are shown for residues in the NRD and TAD (Berjanskii and Wishart, 2005). Lower RCI-S^2 values indicate flexibility, higher RCI-S^2 values indicate rigidity. **(D)** Overlay of ten final Rosetta models guided by the chemical shift, NOE, and RDC data. **(E)** Topology diagram of the NRD and TAD domains. (**F**) Structure of the five-stranded β-sheet. Unambiguously assigned interstrand amide proton-proton NOEs are shown as lines.

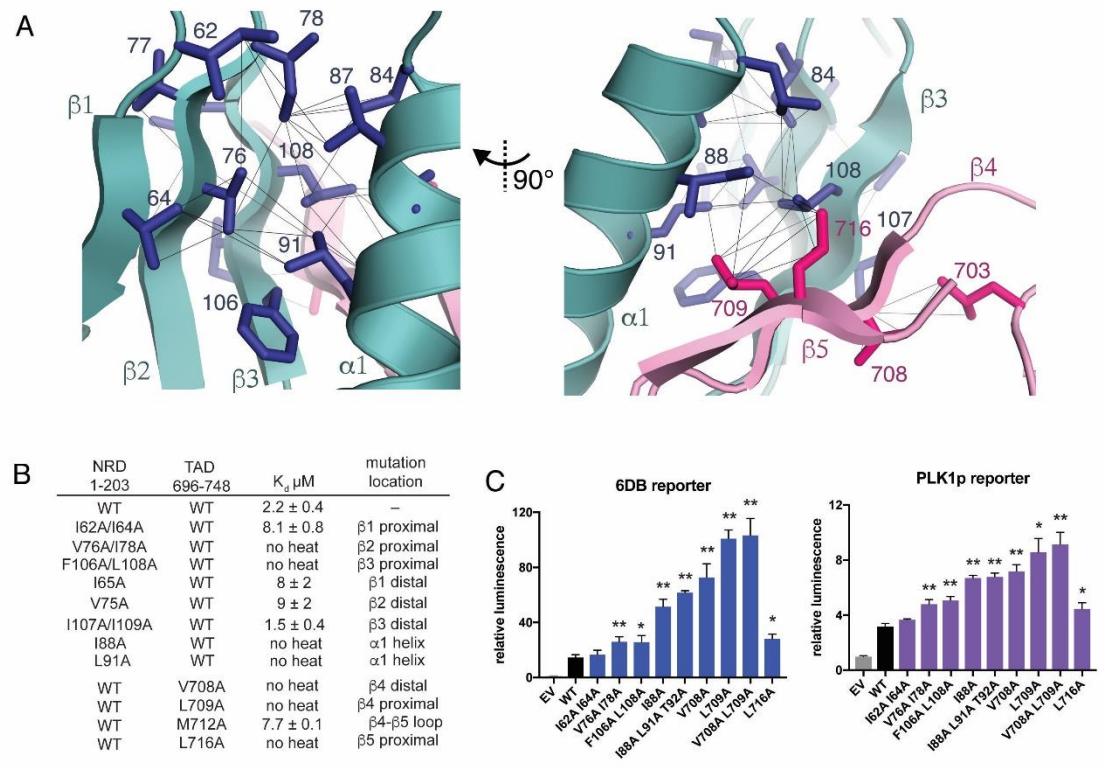
We observed optimal NMR spectra using the protein sequence from zebrafish, deleting an internal loop in the NRD (residues 21-41 in the zebrafish sequence, Figure 2A), cleaving the fusion linker, and uniformly deuterating the nonexchangeable hydrogen positions. We assigned 64% of the backbone H^N, N^H, Cα, and Cβ chemical shifts in this construct using triple-resonance backbone correlation spectra with TROSY readout. Using TALOS-N (Shen and Bax 2015; Shen et al. 2009), we calculated the secondary structure index (SSI) and estimated backbone order parameter (RCI-S^2, 0 is total disorder and 1 is fully rigid) for the assigned regions of both domains. We find significant structural order within a set of residues including sequences from both the NRD and TAD. Importantly, within this ordered region, the backbone chemical shifts for 71 out of 75 non-proline residues were assigned. Notably, the SSI analysis suggests that a stretch of residues in the TAD adopts a β-hairpin conformation, which contrasts the helical TAD structures typically observed in complexes with co-activator domains (De Guzman et al. 2006; Goto et al. 2002; Krois et al. 2016; I. Radhakrishnan et al. 1997; Zor et al. 2004).

To build a model of the core NRD-TAD structure, we prepared perdeuterated protein samples with isoleucine, leucine, and valine (ILV) methyl sidechain $^{13}C/^{1}H$ labels. We performed a combination of isotopomer-selective TOCSY experiments and several NOESY experiments to assign and validate the resonances of ILV methyls and generate a set of NOE-based distance restraints for structure calculations (see Methods) (Otten et al. 2010). We then combined the chemical shifts, NOE restraints, and RDCs to generate a set of structures using customized RASREC-Rosetta calculations, as described in Methods. We included only the core, structured sequences of each domain in the calculation. Sequences outside the core region are likely disordered, as suggested by no observable NOEs and low order parameters for assigned residues in the flanking regions. The structural ensemble of the NRD-TAD complex, which consists of ten top scoring models based on Rosetta energy function and good overall fit to the experimental data, showed high convergence with heavy atom root mean square displacements of 0.48Å for core residues. The observed backbone

conformation in these calculated models match TALOS-N chemical shift predictions of secondary structure and fits experimental RDC data well. The core structured elements in the NRD and TAD correlate well with the sequences of highest conservation in those domains, and nearly all the residues that are key for forming the interface are conserved.

The NRD-TAD structure consists of a five-stranded pleated β-sheet and a single α-helix. Three of the beta strands (β1-β3) are from sequences in the NRD, and two additional strands are from sequences in the TAD (β4-β5). The amphipathic helix is an insertion between the parallel β2 and β3 strands in the NRD. One face of the helix packs against the β-sheet to form the hydrophobic core of the structure. Sidechains from β-strands in both the NRD (I64, V76, I78, F106, and L108, human sequence numbering) and TAD (L709 and L716) form an extended, buried interface through highly specific, experimentally confirmed interactions with helix residues (I84, I87, I88, and L91) (Figure 3A). The fact that both the NRD and TAD contribute essential residues to the hydrophobic core suggests the requirement of an association for forming the observed structure of both domains. We explore this idea further below.

The structured region of the TAD consists of a 12 amino acid sequence that adopts a β-hairpin conformation and binds the NRD by extending the β-sheet. The NRD-TAD interface therefore consists of interstrand backbone hydrogen bonds between NRD β3 and TAD β4 and several van der Waals contacts between sidechains in those β-strands and the NRD helix. The backbone hydrogen-bonding network is supported by unambiguously assigned interstrand amide-amide NOE cross-peaks, and, likewise, the sidechain interactions are supported by methyl-methyl NOEs. Sidechain contacts at the interface are observed between I88, L91, F106, I107, and L108 in the NRD and L703, V708, L709, and L716 in the TAD. Interestingly, even when interacting with the NRD, ~20% of the TAD is structurally well defined, while the majority of the TAD remains intrinsically disordered. We propose that this small, structurally plastic region of the TAD is key for the regulation of FoxM1 activity.



NRD 1-203	TAD 696-748	K_d μM	mutation location
WT	WT	2.2 ± 0.4	–
I62A/I64A	WT	8.1 ± 0.8	β1 proximal
V76A/I78A	WT	no heat	β2 proximal
F106A/L108A	WT	no heat	β3 proximal
I65A	WT	8 ± 2	β1 distal
V75A	WT	9 ± 2	β2 distal
I107A/I109A	WT	1.5 ± 0.4	β3 distal
I88A	WT	no heat	α1 helix
L91A	WT	no heat	α1 helix
WT	V708A	no heat	β4 distal
WT	L709A	no heat	β4 proximal
WT	M712A	7.7 ± 0.1	β4-β5 loop
WT	L716A	no heat	β5 proximal

Figure 3.3: Interactions stabilizing the NRD-TAD hydrophobic core and interface. (A) Hydrophobic sidechains forming the structural core of the NRD-TAD complex. Human amino acid numbering is indicated. Unambiguously assigned ILV methyl-methyl NOEs are shown as lines. **(B)** ITC measurements of the NRD-TAD binding affinity using the indicated WT or mutant domains. Mutations were chosen on the side of the β-sheet that is either proximal or distal to the α-helix. (**C)** Luciferase reporter assays of FoxM1 transactivation activity. Reporter plasmids containing the luciferase gene downstream of either six repeats of a FoxM1 responsive element (6DB, left) or the PLK1 promoter sequence (PLK1p, right) were co-transfected with WT or mutant FoxM1 into U2OS cells. EV is empty vector. Significant differences in the relative luminescence from WT are indicated with asterisks: * $p < 0.05$, ** $p < 0.01$ (using two-tailed student's t-test).

3.2.3. The NRD-TAD has a hydrophobic core and disruption of the interface leads to heightened FoxM1 transcriptional activity

To probe the structural role of the NRD-TAD interface in repressing FoxM1 transactivation, we first tested the effects of mutations in the NRD and TAD on the interdomain association using the ITC assay with human FoxM1 domains. For these experiments, we used the TAD (696-748) and a longer NRD (1-203), which were the most stable constructs containing each domain in solution and the simplest to purify. We

expressed and purified NRD constructs (residues 1-203) containing mutations in each of the three β-strands. These mutations, which replace hydrophobic sidechains for alanine, were made to residues on either the face of the β-sheet that interact with the helix (proximal) or the face pointing away from the helix (distal). We find that mutations on the β-sheet face that is proximal to the helix all inhibit binding with the TAD (residues 696-748), with mutations on the two strands closest to the TAD (V76A/I78A in β2 and F106A/L108A in β3) having the greatest effects. We find that mutations to the hydrophobic face of the NRD helix (I88A and L91A) also disrupt TAD binding. In contrast, mutations to the distal side of the NRD β-sheet only result in a modest decrease in affinity (I65A or V75A) or no change in affinity (I107A/I109A). We also substituted alanines for sidechains in the TAD near the NRD interface. We found that three mutations have strong effects on binding (V708A, L709A, L716A), while mutation at one sidechain that points toward the distal side of the sheet (M712A) has a modest effect. We next tested the effects of mutations to the NRD-TAD interface on FoxM1 activity in U2OS osteosarcoma cells using a luciferase reporter. We expressed WT and mutant FoxM1 together with a plasmid that contains 6 tandem Forkhead-response elements (6DB) or the promoter of PLK1 (PLK1p), a FoxM1 target gene, upstream from the luciferase gene. As previously described, luciferase activity increases upon expression of WT FoxM1 compared to transfection of empty vector, which reflects the ability of FoxM1 to transactivate luciferase expression from the promoters in the reporter plasmid (Anders et al. 2011; Laoukili et al. 2005). We find that this activity is further increased upon expression of FoxM1 harboring mutations that destabilize the NRD-TAD interface. The cell reporter data generally correlate well with our *in vitro* ITC binding data. For example, a β1 strand mutant (I62A/I64A), which only produces a modest loss of binding affinity, does not significantly change FoxM1 activity in the cell assay. In contrast, mutations closer to the interface in NRD strands β2 and β3, the NRD helix, and the TAD have strong effects. We conclude that the WT FoxM1 activity in this assay is mitigated by autorepression and that, by destabilizing the NRD-TAD structure and association, these mutations inhibit autorepression and result in higher activity. One

interesting exception to the observed correlation between the biochemical and cellular assays is the L716A mutation. This mutation results in complete loss of affinity but has a more modest activating effect in the luciferase assay compared to other TAD mutations. We explore below an additional role for this residue in activation through recruitment of CBP/p300 co-activator.

3.2.4. Disruption of CBP binding motif decreases relief of repression

The structures of several TAD sequences bound to CBP or p300 KIX and TAZ2 have been determined, and it is found that the intrinsically disordered TADs invariably adopt helical conformations when associated with co-activator (De Guzman et al. 2006; Goto et al. 2002; Krois et al. 2016; I. Radhakrishnan et al. 1997; Goto et al. 2002). Binding typically entails contacts from hydrophobic residues along the face of one or more short amphipathic helices in the TAD. Motifs such as ϕ-X-X-ϕ-ϕ or ϕ-ϕ-X-X-ϕ (ϕ is a bulky hydrophobic residue and X is any residue) are commonly observed in the TAD interacting sequences. Two sequences in the FoxM1 TAD contain such a motif and appear amenable to forming amphipathic helices. We find that both of these sequences are required for TAZ2 binding. Notably, the predicted binding sequence around 713-726 overlaps with the sequence that forms the β-hairpin in binding the NRD in the repressed conformation. We tested a L716A TAD mutant and found no detectable binding to TAZ2. The importance of L716 for CBP association explains how NRD binding inhibits CBP association and likely explains why the L716A mutation did not result in similar increased FoxM1 activity in the luciferase assay as other mutations in the TAD. The mutation disrupts both NRD inhibition and activation through CBP recruitment.

3.2.5. FoxM1 TAD bound to CBP by NMR

To test the possibility of determining the secondary and/or tertiary structure of the TAD bound by CBP we used NMR and assigned the partial backbone of the FoxM1 TAD bound by CBP-TAZ2. We had previously sought to determine the backbone assignments and

subsequent secondary structure of the TAD bound by CBP-KIX (unpublished data), but due to tighter binding by TAZ2 we opted for structural analysis of the TAZ2 bound TAD. We were able to assign 64% of backbone residues, 55% of Cα atoms, and 45% of Cβ atoms (Table 3.1). There is a substantial portion of the middle of the TAD that is entirely unassigned and is not visible by the 3D NMR acquisition parameters, specifically zebrafish residues 597-605, which correspond to human 719-727, a highly conserved region that we propose has critical binding residues based on mechanistic conservation of hydrophobic binding of TADs to CBP (De Guzman et al. 2006; Goto et al. 2002; F. Wang et al. 2012).

Residue	H	N	Cα	Cβ
568 Gly				
569 Glu				
570 Phe	8.53	121.41	57.97	41.13
				39.50
571 Gly	8.35	111.07	44.61	
572 Ala	8.11	123.91		19.45
	8.11	123.91		
573 Ala				
574 Asn	8.33	122.79	54.94	38.98
	8.31	117.44	51.64	38.48
	8.14	117.35		
574 Asn				
575 Arg	7.83	125.85	57.39	
575 Arg	8.24	121.56	57.56	30.99
	7.83	125.55	56.31	31.52
				31.58
576 Ser				
577 Leu	7.91	129.83	56.78	43.35
578 Thr				
579 Glu	8.24	122.70	56.92	
580 Gly	8.49	110.37	45.35	
580 Gly	8.34	109.29		
581 Phe	8.00	120.14	57.88	38.88
	8.12	120.02	57.63	
581 Phe				39.10
582 Val				
583 Leu	8.41	119.33	57.02	30.21
	8.40			39.58
584 Asp				
585 Thr	8.00	112.64	61.65	69.95
586 Met	7.96	127.54	57.24	33.69
587 Asn				
588 Asp				
589 Ser	8.28	115.85	60.07	
590 Leu				
591 Ser	8.17	116.15	63.72	
	8.17	116.15	58.42	
		116.14		
592 Lys	7.66	128.46	58.55	30.29
593 Ile				
594 Leu				
595 Val				
596 Asp	8.24	126.24	55.13	42.72
597 Ile				
598 Ser				
599 Phe				
600 Ser				
601 Gly				
602 Leu				
603 Glu				
604 Asp				
605 Glu				
606 Asp				
607 Leu	8.36	121.42	54.70	41.37
608 Gly		107.69	46.48	
609 Met	8.16	118.73	55.61	33.02
610 Gly	8.43	108.55	45.76	
		108.58		
611 Asn	8.24	118.51	53.29	38.97
612 Ile	7.93	120.72	60.75	40.44
614 Trp				
615 Ser	8.36	117.80	58.38	64.02
616 Gln				
617 Phe	8.42	122.49	57.84	39.53
618 Ile				
619 Pro				
620 Glu	8.43	120.90	56.44	30.17
621 Leu				
622 Lys	7.89	127.85	57.56	33.96

Table 3.1: FoxM1 TAD bound by CBP-TAZ2 chemical shift assignments. The FoxM1 TAD and all assignments are categorized by atom type; H, amide proton, N, backbone nitrogen, Cα and Cβ carbon atoms. Values are in ppm in the respective dimension.

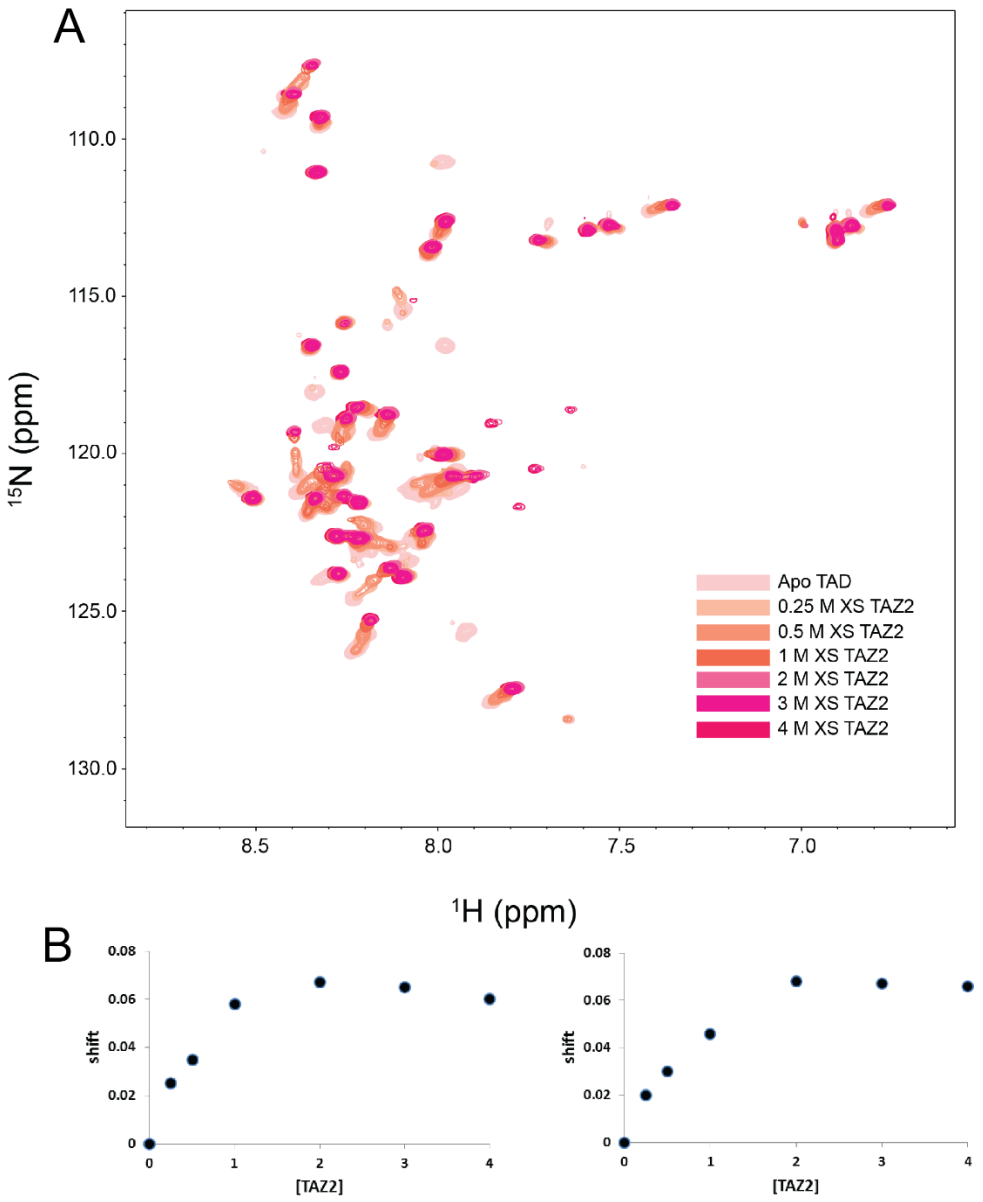


Figure 3.4: The FoxM1 TAD and CBP by NMR. (A) HSQC of ^{15}N **Dr** FoxM1 TAD at 100 µM is titrated with molar equivalents of unlabeled TAZ2 as indicated by the key. While many residues are visible by HSQC, a significant number fall into intermediate exchange and additional residues are not visible in 3D data. **(B)** Binding analysis of two representative fast exchange residues in the bound HSQC show a plateau of chemical shift perturbation at a 2M equivalent of TAZ2:TAD.

We first determined the ratio at which the FoxM1 TAD is saturated with TAZ2. To do this we titrated unlabeled TAZ2 into 100 μM ^{15}N labeled TAD and graphed peaks in fast exchange. We found that at a 2M equivalent of TAZ2 (200 μM) to TAD we saw a plateau of chemical shift perturbation of residues in fast exchange, indicating that the TAD is saturated at 2M excess (Figure 3.4B). Consequently, all experiments moving forward were conducted at 2M excess of TAZ2 to FoxM1 TAD. Due to protein degradation and intermediate exchange we were unable to assign sufficient residues for 3D structure determination. There is a native linker fusion construct of TAZ2-TAD with an N terminal GST tag that expresses and could be tested for stability and signal (**3.4 materials and methods**).

3.2.6. The FoxM1 TAD has α-helical propensity in a CBP bound state

The FoxM1 TAD binds to CBP TAZ2 and is partially visible by NMR in a bound state. Transcription factors that bind to CBP domains often adopt α-helical structure upon binding through a conserved hydrophobic interaction. Due to the conservation of both amino acid sequence in these hydrophobic sequences and conservation of mechanism we also expect the FoxM1 TAD to adopt helical propensity (Figure 3.5B). In addition, there are residues in the bound HSQC that perturb upfield in the ^{1}H dimension, indicative of α-helical structure formation (Figure 3.5A). The FoxM1 TAD with the TEV linker site has 54 non-proline residues. In the bound HSQC we see 48 peaks and it is expected that some of these peaks are due to protein degradation over time. Though overall the bound state seems to remain primarily disordered, an interesting region of the FoxM1 TAD moves upfield in a manner that is indicative of α-helical propensity.

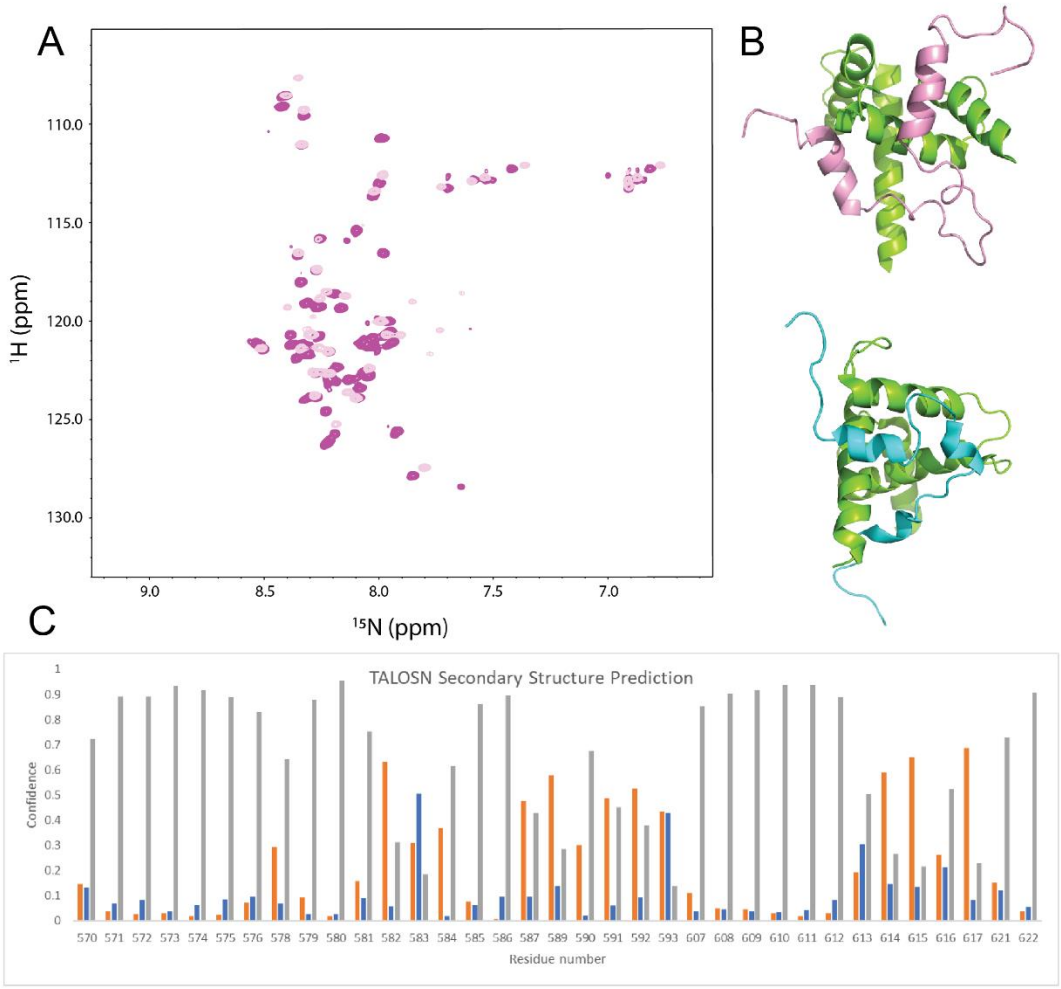


Figure 3.5: CBP bound TAD shows α-helical propensity. (A) NMR HSQC spectra show the unbound FoxM1 TAD (dark purple) overlaid with the bound FoxM1 TAD (light pink). Notably, we see chemical shift perturbations in the proton dimension moving upfield upon TAZ2 interaction. **(B)** TADs typically adopt α-helical confirmations upon binding to TAZ2. Shown here are representative structures of TAD bound TAZ2 domain; top, TAZ2 bound by p53 (PDB ID 5HPD), bottom, TAZ2 bound by E1A (PDB ID 2KJE). **(C)** TALON-N was used to predict secondary structure. Residue number on the x-axis corresponds to zebrafish FoxM1 TAD and secondary structure predictions are colors; α-helix orange, β-sheet blue, disorder gray.

To begin to ask questions regarding secondary structure during TAZ2 bound state of the FoxM1 TAD we assigned the protein amide backbone using triple resonance experiments. Of the available 48 of 54 peaks visible to assign 31 are assigned (64%

assigned residues). TALOS-N was used to predict secondary structure based of the TAZ2 bound TAD based on chemical shifts as perturbed from random coil (Figure 3.5C). The FoxM1 TAD in a TAZ2 bound state has regions where the TAD tends to have an equal if not slightly larger probability of being in an α-helical state, specifically residues 587 – 593 and 614 – 621. It is worth noting that one of the regions of the TAD that corresponds to the hydrophobic binding motif that commonly binds CBP regions is not visible by 3D NMR in the bound state and therefore could not be assigned nor predicted. While this extremely limits our investigation, we still believe based on the overall data that the FoxM1 TAD likely samples an α-helical state. This will be extended upon in the discussion.

3.2.7. FoxM1 TAD is unstructured in a phosphorylated state

To further probe the structure of the TAD alone and the effects of Plk1 phosphorylation, we collected NMR data and assigned the backbone amide chemical shifts for the zebrafish FoxM1 TAD (residues 571-623, which corresponds to human 696-748), using both unphosphorylated and Plk1-phosphorylated samples. 47 out of 50 of the non-Pro residues in the TAD and phosphorylated TAD were assigned. Using TALOS-N as above, we calculated the RCI-S^2 order parameter for residues in both the phosphorylated and unphosphorylated TAD. The data support the conclusion that both the phosphorylated and unphosphorylated isolated TAD are primarily unstructured. These results in comparison with the NMR data for the NRD-TAD complex suggest that the β-hairpin structure of the TAD is adopted upon binding to the NRD.

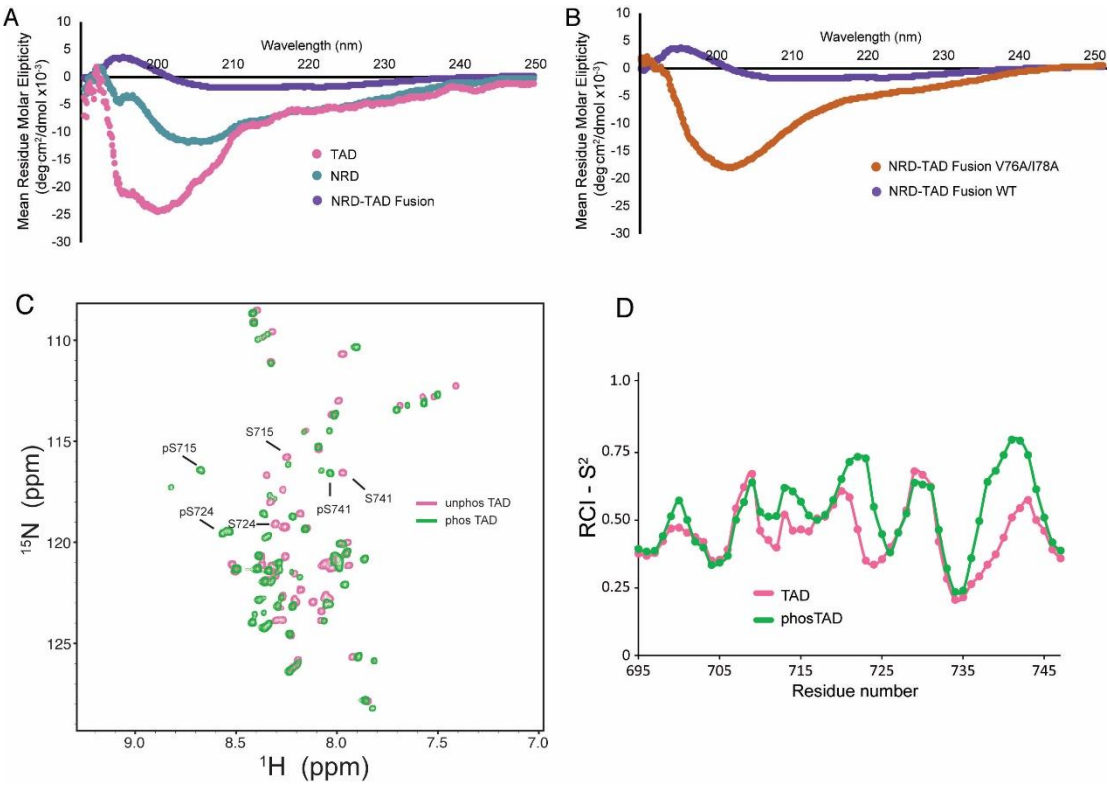


Figure 3.6: The Plk1 phosphorylated TAD is intrinsically disordered. (A, B) CD spectra of the indicated purified proteins**. (C)** 2D ^{1}H-^{15}N HSQC spectra of the zebrafish FoxM1 TAD (corresponding to residues 696-748 in the human protein) either unphosphorylated (pink) or phosphorylated (green) recorded at 25°C at 800 MHz. Sequence specific assignments (examples shown for three Plk1-phosphorylated serines) were made using backbone triple resonance correlation spectra. **(D)** RCI-S^2 order parameter plot of assigned residues in the free TAD and Plk1-phosphorylated TAD.

3.2.8. Conclusions

Detailed in **Chapter 2** is the mechanism of FoxM1 activation and relief and repression in a phosphorylation dependent manner. Here in **Chapter 3** we add onto the mechanism by detailing the core of the NRD-TAD association as well as the structural rearrangements in the TAD. These structural rearrangements occur in a phosphorylation dependent manner with the phosphorylation of S715 relieving the NRD sequestration of the TAD and allowing CBP to bind. This data was detailed in **Chapter 2, Figure 2.5**. Here we show that FoxM1 TAD has a hydrophobic core that can be destabilized by mutations and that these destabilizing mutations lead to increased FoxM1 transcriptional activity as monitored by

luciferase activity (Figure 3.3). This indicates to us that the hydrophobic core has a prominent role in the maintenance of the NRD-TAD association and subsequently the transcriptional activity of FoxM1. In addition to discovering the NRD-TAD core, we show that FoxM1 undergoes significant structural rearrangements when transitioning from the repressed state to the active CBP bound state. Of note, we show the NRD and TAD to be both intrinsically disordered in isolation, but upon binding form structure (Figure 3.1, Figure 3.2). The TAD exhibits a β-sheet structure when bound by NRD, intrinsic disorder in isolation regardless of phosphorylation status, and has α-helical propensity when bound by CBP (Figure 3.5, Figure 3.6). These findings compliment the work of **Chapter 2** and progress our knowledge of cell cycle regulation, the structural dynamics of eukaryotic transcription factors, and FoxM1 biology.

3.3 Discussion

Eukaryotic transcription factors almost invariably contain large regions of intrinsic structural disorder, which facilitate protein-protein interactions for gene activation, posttranslational modifications for regulation, and control over nuclear localization (Minezaki et al. 2006; Wright and Dyson 2015). Whereas structural disorder is required for function, it follows that the induction of structure could be used to negatively regulate transcription factor activity by restricting accessibility, particularly of the transactivation domain. Indeed, our results show that the NRD of FoxM1 is able to bind the TAD and induce a structured conformation that is incompatible with its binding to co-activator protein. Interestingly, the repressed TAD has a β-hairpin structure, while the CBP bound state likely contains α-helical structures and involves a TAD sequence near the S715 phosphorylation site that overlaps with the NRD-binding sequence. Thus, FoxM1 regulation entails secondary structure switching of the TAD between strand, coil, and helical structures.

We find that S715 phosphorylation destabilizes the NRD-TAD association and that the dissociated TAD is intrinsically disordered and capable of binding CBP. Phosphorylation has been observed to control structural transitions as a means to regulate other intrinsically disordered proteins. For example, both the transcription factor Ets-1 and the translation regulator 4E-BP2 undergo disorder-to-order transitions upon phosphorylation, while the nucleophosmin protein dissociates from a structured pentamer to a disordered monomer upon phosphorylation (Bah et al. 2015; Mitrea et al. 2014). FoxM1 demonstrates a new example in which the order-to-disorder transition occurs coincident with modulation of an intramolecular association between domains. This plasticity of disordered domains and the ability to regulate the plasticity through posttranslational modifications explains why intrinsically disordered proteins are so well suited to regulate biological function.

Unexpectedly, our data indicate that in the active FoxM1 conformation, in which phosphorylation inhibits the repressive NRD-TAD association, the NRD is largely disordered as well as the TAD. We propose that this additional disorder may be important to increase

conformational flexibility within the context of chromatin, to promote regulation of FoxM1 stability, or to contribute to the formation of low complexity domain condensates as recently described (Chong et al. 2018; Laoukili et al. 2008; Liu et al. 2006; Minezaki et al. 2006; Park, Costa, et al. 2008; X. Wang et al. 2017; Wright and Dyson 2015). While several transcription factor NRDs have been characterized (W. Y. Kim et al. 1999; Park, Wang, et al. 2008; Ramsay and Gonda 2008; Shi, Kroeger, and Morimoto 1995; Spengler and Brattain 2006; Wierstra and Alves 2006), the idea that NRDs may appear in regions of intrinsic disorder should motivate the identification of additional "hidden" NRDs that adopt structure only upon interaction with their target.

Like many cell division regulatory proteins, FoxM1 undergoes cell-cycle dependent multisite phosphorylation. While multiple Cdk and Plk1 phosphorylation events have been implicated in FoxM1 activation, our results demonstrate that phosphorylation of one specific Plk1 site (S715) is directly responsible for freeing the TAD from sequestration by the NRD. This result clarifies an indirect role for Cdk in driving FoxM1 activity through priming the CSR for Plk1 docking and further phosphorylation of the TAD (Fu et al. 2008). The idea that different phosphorylation events have specific and distinct roles is in contrast to several proposed models for multisite phosphorylation in the cell cycle, in which a threshold aggregate of redundant phosphorylation events drives a change in protein activity (Harvey et al. 2005; S. Y. Kim and Ferrell 2007). Our observation of specificity in the effects of FoxM1 phosphorylation more resembles what has been proposed for the retinoblastoma protein, in which specific phosphorylation events drive distinct structural changes or protein-protein interactions (Rubin 2013).

The structural picture revealed here of FoxM1 repression provides novel mechanistic insights into transcription factor regulation and may motivate novel cancer therapeutics. It has been concluded that FoxM1 inhibition would significantly impact our treatment of several cancers that express high levels of the protein (Koo et al., 2012; Myatt and Lam, 2007; Raychaudhuri and Park, 2011). However, consistent with the challenges of targeting

transcription factors with chemotherapeutics, only few reports have described potential candidate molecules (Gormally et al. 2014; S. K. Radhakrishnan et al. 2006). The identification of a structured, repressed conformation suggests the possibility of developing molecules that bind and stabilize the repressive NRD-TAD association or target FoxM1 for degradation.

3.4 Materials and Methods

Protein Expression

The zebrafish FoxM1 TAD fused to mouse CBP-TAZ2 with a native FoxM1 linker was expressed in and purified from *E. coli* as N-terminal GST fusion proteins with TEV cleavage sites. Cells were induced in mid-log phase with 1 mM IPTG, cells were grown for 3-4 hours at 25 °C. Protein was purified from lysates with glutathione sepharose affinity chromatography. Fusion was then cleaved with TEV protease overnight against dialysis buffer (25 mM Tris 8, 200 mM NaCl, 5 mM DTT, 10% glycerol v/v) and once again the next morning. Cleaved fusion was then passed over glutathione sepharoto remove free GST, concentrated, and run over Superdex-75 (GE Healthcare) into 20 mM HEPES pH 7.5, 150 mM NaCl, 5% glycerol.

Circular dichroism

Circular dichroism spectra of the FoxM1 proteins, prepared in 20 mM sodium phosphate and 50 mM NaCl buffer (pH 7.0), were measured on a JASCO J-1500 spectrometer using a 1 mm path length quartz cuvette. Data were collected every 0.1 nm from 190 to 300 nm using a scanning speed of 50 nm/min, a digital integration time of 4 s, and a bandwidth of 4 nm. Eight sets of data were collected for each protein. Protein concentrations ranged from 35 µM to 10 µM and were measured using absorption at 280 nM.

Protein expression for NMR

Zebrafish FoxM1 (DrFoxM1) transactivation domain (G571-K623) and NRD-TAD fusion (Figure 2-figure supplement 1A) were expressed and purified from *E. coli* as above except the cells were grown in M9 medium supplemented with ^{15}N ammonium chloride and ^{13}C glucose. For isoleucine, leucine, and valine specific isotope labeling the cells were grown as above in deuterated M9 medium supplemented with deuterated ^{12}C glucose and the specific precursors added 30 minutes before induction as described (Tugarinov and Kay 2003). For the isotopomer-selective TOCSY experiment, DrFoxM1 was grown in D_2O M9-

media using ^{13}C glucose (^{1}H,^{13}C-glucose). For the ILV sample, residues L19, L104, C87, L569, V571, L622 were mutated to alanine to reduce the number of overlapped peaks in the methyl spectra and to prevent disulfide formation. For each NMR sample, the protein was purified as described in **Chapter 2** and cleavage of the TEV linker was monitored by SDS-PAGE.

Nuclear magnetic resonance data collection and assignments

FoxM1 NRD-TAD fusion

NMR experiments for resonance assignment were performed on a Bruker Avance III HD 800-MHz spectrometer equipped with a cryogenically cooled probe head. All samples were prepared in a buffer containing 20 mM sodium phosphate pH 6.3, 100 mM KCl, and 5% (v/v) D_2O. The NMR spectra for backbone resonances assignments were collected using a 270 µM uniformly ^{13}C, ^{15}N–labeled deuterated DrFoxM1 NRD-TAD. Sequence-specific backbone resonance assignments for DrFoxM1 NRD-TAD were determined using all TROSY-HSQC, TROSY-HNCO, TROSY-HN(CA)CO, TROSY-HNCA, TROSY-HN(CO)CA, TROSY-HNCB, and TROSY-HN(COCA)CB experiment supplied by Bruker BioSpin. NMR spectra for methyl sidechain assignments were collected using 270 µM deuterated uniformly ^{15}N-labeled, methyl site specific ^{13}C-labeled protein. Methyl sidechain assignments were determined using an isotopomer-selective TOCSY and SOFAST NOESY, HMQC, and methyl-HSQC experiments (Otten et al. 2010; Rossi et al. 2016). Data from the protein samples with methyl specific labels was collected using SOFAST pulse sequences (Rossi et al. 2016), including amide to amide NOESY (H_N-NH_N and N-NH_N), amide to methyl (H_NH_{Aro}-C_MH_M and C_M-NH_N) and methyl to methyl (H_M-C_MH_M and C_M-C_MH_M) SOFAST NOESY experiments all recorded with a recycle delay of 0.2 sec and an NOE mixing time of 300 msec.

FoxM1 TAD

NMR experiments for resonance assignment were performed on a Bruker Avance III HD 800-MHz spectrometer equipped with a cryogenically cooled probe head. All samples were prepared in a buffer containing 20 mM Sodium Phosphate pH 6.3, 100 mM KCl, and 5% (v/v) D_2O. The NMR spectra for backbone resonances assignments were collected using a 450 µM uniformly ^{13}C, ^{15}N–labeled DrFoxM1 TAD protein. NMR labeled TAD protein was phosphorylated by Plk1 kinase domain as described above. Sequence-specific backbone resonance assignments for DrFoxM1 TAD were determined using HSQC, HNCO, HNCACB, CBCA(CO)NH, and C(CO)NH experiment supplied by Bruker BioSpin. Sequence-specific backbone resonance assignments for phosphorylated DrFoxM1 TAD were determined using HSQC, HNCO, HNCACB, and CBCA(CO)NH experiments supplied by Bruker BioSpin.

FoxM1 TAD-TAZ2

NMR experiments for resonance assignment were performed on a Bruker Avance III HD 800-MHz spectrometer equipped with a cryogenically cooled probe head. All samples were prepared in a buffer containing 20 mM Sodium Phosphate pH 6.3, 100 mM KCl, and 5% (v/v) D_2O. The NMR spectra for backbone resonances assignments were collected using a 1µM uniformly ^{13}C, ^{15}N–labeled DrFoxM1 TAD protein and incubated with 2M excess unlabeled TAZ2. Sequence-specific backbone resonance assignments for DrFoxM1 TAD-TAZ2 were determined using HSQC, HNCO, HNCACB, CBCA(CO)NH, and C(CO)NH, HBHA(CO)NH experiment supplied by Bruker BioSpin.

Residual Dipolar Coupling

The backbone D_{NH} (NH) dipolar couplings used for RASREC-Rosetta structure modeling were measured using uniformly ^{15}N-labeled deuterated FoxM1 NRD-TAD protein. The NMR sample was made by mixing DrFoxM1 NRD-TAD (250 µM final concentration) with Pf1 phage (12.5 mg/mL final concentration) and 10% D_2O (Hansen et al., 1998). RDCs were

collected on a Varian INOVA 600 MHz spectrometer using J modulation experiments similar to those described (Tjandra et al., 1996). The D_{NH} coupling experiment was performed with the ILV NRD-TAD sample containing the alanine mutations (Figure 2-figure supplement 1A). A separate set of backbone $D_{NC'}$ (NCO) dipolar couplings were measured using uniformly $^{15}N/^{13}C/^{2}D$ labeled FoxM1 NRD-TAD fusion protein and used for structure validation. This set of RDCs were not used in the structural calculation of the FoxM1 model. The NMR sample was made by mixing DrFoxM1 NRD-TAD (250 µM final concentration) with Pf1 phage (12.5 mg/mL final concentration) and 10% D_2O (Hansen et al., 1998). RDCs were collected on a Varian INOVA 600 MHz spectrometer using J modulation experiments similar those described previously (Liu and Prestegard, 2010). The $D_{NC'}$ coupling experiment was performed with the uniformly $^{15}N/^{2}D$-labeled NRD-TAD fusion sample (no alanine mutations) used for backbone assignments.

All NMR data were processed with NMRPipe and NMRDraw (Delaglio et al. 1995). Chemical-shift assignments were made with SPARKY (https://www.cgl.ucsf.edu/home/sparky/).

Structure modeling using RASREC-Rosetta

Structural models of the NRD-TAD complex were calculated using RASREC-Rosetta (Nerli and Sgourakis 2019). RASREC-Rosetta is a Monte Carlo-based fragment assembly approach that utilizes NMR chemical shifts to guide the conformation search for a near-native structure. Together with NMR chemical shifts, which aid in the selection of accurate secondary structural elements, we utilized NOE and RDC measurements that helped identify the correct fold of the two domain(Tyka et al. 2011). Alongside NMR data, RASREC-Rosetta uses optimized algorithms across six stages of resampling in a parallelized manner to achieve high structural convergence. During the initial stages of the protocol, various β-sheet topologies are sampled. In the subsequent stages, fragments derived from (i) high-resolution X-ray structures, and (ii) preliminary low-resolution conformations (from the initial sampling

stages), are applied to intensify and finalize the folds of a target protein. In the final stages of the protocol, the low-resolution models generated during the initial and intermediate stages are refined in the Rosetta force field to produce high-resolution structures.

Structure calculations were set up with automated Python scripts available at the CS-Rosetta website (https://csrosetta.chemistry.ucsc.edu). Prior to setting up these calculations, we (i) removed flexible end regions in the target sequence based on TALOS-N RCI-S^2 predictions, and (ii) used the trimmed target sequence and chemical shift values to pick structural fragments of amino acid lengths 3 and 9 (standard lengths). After these steps, we used the protein sequence, structural fragments, chemical shift, NOE and RDC measurements as input to the RASREC-Rosetta protocol. From a set of 100 models generated by RASREC-Rosetta in its final stage, we selected 30 lowest energy models from which, we filtered ten converged structures that fit the experimental RDC data. We subsequently refined the final ensemble twice (first, using NOE and RDC data sets and second, without any data sets to eliminate heavy bias from NMR data) using Rosetta's relax protocol (Tyka et al. 2011). The structures of NRD-TAD domains were calculated by treating the protein as a single polypeptide chain with the TEV site as a linker, which was later removed from the models.

To calculate the structural models of the FoxM1 NRD-TAD domains, we used a total of 64 NOE distance restraints derived from highly sensitive SOFAST-based experiments recoded with short inter scan delays (200 msec) and long (300 msec) mixing times. These distance restraints consist of (i) 14 amide to amide, (ii) 11 amide to methyl, and (iii) 39 methyl to methyl NOEs. The observed intensities of the NOEs can be affected by distance-independent processes such as T1 relaxation and spin diffusion during the long NOE mixing time. Accordingly, we considered several additional parameters, alongside the signal intensities of the NOEs (relative to their diagonals), to calibrate upper distance bounds for all the three classes of NOE restraints described above. In particular, we performed an analysis of distance statistics within β-sheet structures in the PDB and used preliminary models of the

NRD-TAD domains calculated using more generous (7 Å), uniform NOE distance limits as benchmarks. First, we filtered NOEs based on high signal intensities. From a non-redundant set of 5 β-sheet X-ray structures in PDB, we found that anti-parallel β-strands have NOEs between pairs of amide protons within ~3 Å or ~5 Å and parallel β-strands within ~3 Å or ~4 Å. We then used the approximate relation that, NOE signal intensities are inversely proportional to sixth power of distances ($I_{NOE} = c \times r^{-6}$, where I_{NOE} is the NOE signal intensity, c is the proportionality constant and r is the distance), to obtain estimates of upper distance bounds. To determine the proportionality constant, we used the strongest-intensity NOE and approximate distances between the amide protons from β-sheet X-ray structures in PDB. Further, we applied the estimated proportionality constant and measured signal intensities to generate upper distance bounds for other amide-amide NOEs. Similarly, we used preliminary models computed using fixed distance bounds to calibrate distances of amide-methyl and methyl-methyl NOEs. Using this process, we observed that the resulting convergence of NRD-TAD ensemble calculated by RASREC-Rosetta increased progressively, together with the optimization of structural quality parameters such as Rosetta energies and MOLPROBITY scores.

Cell culture

Human osteosarcoma U2OS cells were maintained in Dulbecco's modified Eagle's medium (DMEM) containing 10% fetal bovine serum, 2mM L-glutamine, and 1x Penicillin Streptomycin and split every 2-3 days. Cells tested negative for Mycoplasma contamination using a PCR assay.

Reporter assays were performed using the FoxM1c isoform, which includes 15 amino acids downstream of the DNA binding domain that are absent in FoxM1b. The amino acid sequence of the NRD, CSR and TAD domains are identical in FoxM1c and FoxM1b. For clarity, mutations are indicated using FoxM1b numbering throughout the figures and text.

Mutants were expressed from the pCDNA3 plasmid with and contain an N-terminal FLAG tag: pCDNA3-FOXM1C (WT), pCDNA3-FOXM1C-I62A I64A, pCDNA3-FOXM1C-V76A I78A, pCDNA3-FOXM1C-I88A, pCDNA3-FOXM1C-I88A L91A T92A, pCDNA3-FOXM1C-F106A L108A, pCDNA3-FOXM1C-V723A (V708A in FOXM1b), pCDNA3-FOXM1C-L724A (L709A in FOXM1b), pCDNA3-FOXM1C-V723A L724A (V708A L709A in FOXM1b), pCDNA3-FOXM1C-L731A (L716A in FOXM1b), pCDNA3-FOXM1C-S730A (S715A in FOXM1b). In co-expression experiments with Plk1, Plk1 was expressed from pRcCMV myc-Plk1 wt (a gift from Erich Nigg) (Golsteyn et al., n.d.). The day prior to transient transfections, $2x10^5$ U2OS cells were seeded into 12-well plates in antibiotic-free medium (DMEM/ 10%FBS/L-glutamine). Cells were then transfected with Lipofectamine 2000 Reagent (Invitrogen 11668-019) according to the manufacturer's protocol with 650ng pGL3-6DB-reporter or pGL3-PLK1 promoter reporters (a kind gift from Piotr Sicinski, (Anders et al. 2011)), 650ng pcDNA3-FOXM1C (WT or mutant), and 10ng of pCMV-Renilla luciferase. In experiments that assayed activation by Plk1, 160ng of pRcCMV myc-Plk1 wt or an empty vector control also included. Media was refreshed 4 hours post-transfection. Cell lysates were prepared 25 hours post-transfection using the Promega Dual Luciferase Reporter Assay System kit (Promega, E1960) and luminescence was measured on a Promega Glo Max. Relative luminescence was determined by normalizing the Firefly luciferase activity (expressed by pGL3 reporter plasmids) activity to Renilla Luciferase (transfection efficiency control). Three technical replicate transfections were performed in each experiment and each experiment was carried out three times (biological replicates). Analysis was performed in Excel and GraphPad Prism software.

Western blot and cell cycle analysis

The day prior to transient transfections, $2x10^6$ U2OS cells were seeded into 10cm plates in antibiotic-free medium (DMEM/ 10%FBS/L-glutamine). Cells were then transfected with Lipofectamine 2000 Reagent (Invitrogen 11668-019) according to the manufacturer's

protocol with 9.5µg pcDNA3-FOXM1 plasmids. Media was refreshed 4 hours post-transfection. Cell lysates were prepared 25 hours post-transfection by resuspending cells in RIPA buffer (150mM NaCl, 1% Triton-X 100, 0.5% Sodium deoxycholate, 0.1% SDS, 50mM Tris-Cl pH 8.0, 5mM Sodium Fluoride, 1mM Sodium Orthovanadate, 80mM β-glycerophosphate, 1µg/mL Leupeptin, 1µg/mL bestatin, 1µM Benzamidine HCl, 1mM DTT) for 30 minutes on ice, followed by centrifugation. Protein concentration was determined using Bio-Rad Protein Assay Dye Reagent (Cat#5000006) and measured on an Eppendorf BioPhotometer Plus. Lysates were added to 4X SDS-PAGE Sample Buffer (0.25 M Tris pH 6.8, 8% SDS, 40% glycerol, 20% β-mercaptoethanol) and heated to 95°C for 5 minutes. 10-20µg total protein was then subjected to SDS–polyacrylamide gel electrophoresis (SDS–PAGE), followed by transfer to nitrocellulose membranes, and Western blotting with the following antibodies: rabbit anti-FoxM1 (Bethyl A301-533A-M), mouse anti-actin (Sigma A1978), mouse anti-Flag (Sigma F1804). For cell cycle analysis, cells were fixed in 70% ethanol at 4˚C overnight. Cells were then centrifuged, washed with PBS, washed with PBS with 0.5% Tween20, then incubated with IFA 5µg/ml RNaseA for 30 minutes at 37˚C. Propidium iodide was added to a final concentration of 50µg/ml. Data were collected using a Guava EasyCyte HT (Millipore) and analyzed with FlowJo software.

3.5 References

Anders, Lars, Nan Ke, Per Hydbring, Yoon J. Choi, Hans R. Widlund, Joel M. Chick, Huili Zhai, et al. 2011. “A Systematic Screen for CDK4/6 Substrates Links FOXM1 Phosphorylation to Senescence Suppression in Cancer Cells.” *Cancer Cell* 20 (5): 620–34.

Bah, Alaji, Robert M. Vernon, Zeba Siddiqui, Mickaël Krzeminski, Ranjith Muhandiram, Charlie Zhao, Nahum Sonenberg, Lewis E. Kay, and Julie D. Forman-Kay. 2015. “Folding of an Intrinsically Disordered Protein by Phosphorylation as a Regulatory Switch.” *Nature* 519 (7541): 106–9.

Chong, Shasha, Claire Dugast-Darzacq, Zhe Liu, Peng Dong, Gina M. Dailey, Claudia Cattoglio, Alec Heckert, et al. 2018. “Imaging Dynamic and Selective Low-Complexity Domain Interactions That Control Gene Transcription.” *Science* 361 (6400): eaar2555.

De Guzman, Roberto N., Natalie K. Goto, H. Jane Dyson, and Peter E. Wright. 2006. “Structural Basis for Cooperative Transcription Factor Binding to the CBP Coactivator.” *Journal of Molecular Biology* 355 (5): 1005–13.

Delaglio, F., S. Grzesiek, G. W. Vuister, G. Zhu, J. Pfeifer, and A. Bax. 1995. “NMRPipe: A Multidimensional Spectral Processing System Based on UNIX Pipes.” *Journal of Biomolecular NMR* 6 (3): 277–93.

Ebert, Marc-Olivier, Sung-Hun Bae, H. Jane Dyson, and Peter E. Wright. 2008. “NMR Relaxation Study of the Complex Formed between CBP and the Activation Domain of the Nuclear Hormone Receptor Coactivator ACTR.” *Biochemistry* 47 (5): 1299–1308.

Fu, Zheng, Liviu Malureanu, Jun Huang, Wei Wang, Hao Li, Jan M. van Deursen, Donald J. Tindall, and Junjie Chen. 2008. “Plk1-Dependent Phosphorylation of FoxM1 Regulates a Transcriptional Programme Required for Mitotic Progression.” *Nature Cell Biology* 10 (9): 1076–82.

Golsteyn, Roy M, Sharon J Schultz, Jiri Bartek, Andrew Ziemiecki, Thomas Ried, and Erich A Nigg. n.d. “Cell Cycle Analysis and Chromosomal Localization of Human Plk1, a Putative Homologue of the Mitotic Kinases Drosophila Polo and Saccharomyces Cerevisiae Cdc5,” 9.

Gormally, Michael V., Thomas S. Dexheimer, Giovanni Marsico, Deborah A. Sanders, Christopher Lowe, Dijana Matak-Vinković, Sam Michael, et al. 2014. “Suppression of the FOXM1 Transcriptional Programme via Novel Small Molecule Inhibition.” *Nature Communications* 5 (1): 5165.

Goto, Natalie K., Tsaffrir Zor, Maria Martinez-Yamout, H. Jane Dyson, and Peter E. Wright. 2002. “Cooperativity in Transcription Factor Binding to the Coactivator CREB-Binding Protein (CBP): THE MIXED LINEAGE LEUKEMIA PROTEIN (MLL) ACTIVATION DOMAIN BINDS TO AN ALLOSTERIC SITE ON THE KIX DOMAIN.” *Journal of Biological Chemistry* 277 (45): 43168–74.

Harvey, Stacy L., Alyson Charlet, Wilhelm Haas, Steven P. Gygi, and Douglas R. Kellogg. 2005. “Cdk1-Dependent Regulation of the Mitotic Inhibitor Wee1.” *Cell* 122 (3): 407–20.

Kim, Sun Young, and James E. Ferrell. 2007. “Substrate Competition as a Source of Ultrasensitivity in the Inactivation of Wee1.” *Cell* 128 (6): 1133–45.

Kim, W Y, M Sieweke, E Ogawa, H J Wee, U Englmeier, T Graf, and Y Ito. 1999. “Mutual Activation of Ets-1 and AML1 DNA Binding by Direct Interaction of Their Autoinhibitory Domains.” *The EMBO Journal* 18 (6): 1609–20.

Krois, Alexander S., Josephine C. Ferreon, Maria A. Martinez-Yamout, H. Jane Dyson, and Peter E. Wright. 2016. “Recognition of the Disordered P53 Transactivation Domain by the Transcriptional Adapter Zinc Finger Domains of CREB-Binding Protein.” *Proceedings of the National Academy of Sciences of the United States of America* 113 (13): E1853–62.

Laoukili, Jamila, Monica Alvarez-Fernandez, Marie Stahl, and René H. Medema. 2008. “FoxM1 Is Degraded at Mitotic Exit in a Cdh1-Dependent Manner.” *Cell Cycle* 7 (17): 2720–26.

Laoukili, Jamila, Matthijs R. H. Kooistra, Alexandra Brás, Jos Kauw, Ron M. Kerkhoven, Ashby Morrison, Hans Clevers, and René H. Medema. 2005. “FoxM1 Is Required for Execution of the Mitotic Programme and Chromosome Stability.” *Nature Cell Biology* 7 (2): 126–36.

Littler, D. R., M. Alvarez-Fernández, A. Stein, R. G. Hibbert, T. Heidebrecht, P. Aloy, R. H. Medema, and A. Perrakis. 2010. “Structure of the FoxM1 DNA-Recognition Domain Bound to a Promoter Sequence.” *Nucleic Acids Research* 38 (13): 4527–38.

Liu, Jiangang, Narayanan B. Perumal, Christopher J. Oldfield, Eric W. Su, Vladimir N. Uversky, and A. Keith Dunker. 2006. “Intrinsic Disorder in Transcription Factors.” *Biochemistry* 45 (22): 6873–88.

Minezaki, Yoshiaki, Keiichi Homma, Akira R. Kinjo, and Ken Nishikawa. 2006. “Human Transcription Factors Contain a High Fraction of Intrinsically Disordered Regions Essential for Transcriptional Regulation.” *Journal of Molecular Biology* 359 (4): 1137–49.

Mitrea, D. M., C. R. Grace, M. Buljan, M.-K. Yun, N. J. Pytel, J. Satumba, A. Nourse, et al. 2014. “Structural Polymorphism in the N-Terminal Oligomerization Domain of NPM1.” *Proceedings of the National Academy of Sciences* 111 (12): 4466–71.

Mujtaba, Shiraz, Yan He, Lei Zeng, Sherry Yan, Olga Plotnikova, Sachchidanand, Roberto Sanchez, Nancy J Zeleznik-Le, Ze’ev Ronai, and Ming-Ming Zhou. 2004. “Structural Mechanism of the Bromodomain of the Coactivator CBP in P53 Transcriptional Activation.” *Molecular Cell* 13 (2): 251–63.

Nerli, Santrupti, and Nikolaos G. Sgourakis. 2019. “CS-ROSETTA.” *Methods in Enzymology* 614: 321–62.

Otten, Renee, Byron Chu, Karla D. Krewulak, Hans J. Vogel, and Frans A. A. Mulder. 2010. “Comprehensive and Cost-Effective NMR Spectroscopy of Methyl Groups in Large Proteins.” *Journal of the American Chemical Society* 132 (9): 2952–60.

Park, H. J., R. H. Costa, L. F. Lau, A. L. Tyner, and P. Raychaudhuri. 2008. “Anaphase-Promoting Complex/Cyclosome-Cdh1-Mediated Proteolysis of the Forkhead Box M1 Transcription Factor Is Critical for Regulated Entry into S Phase.” *Molecular and Cellular Biology* 28 (17): 5162–71.

Park, H J, Z Wang, R H Costa, A Tyner, L F Lau, and P Raychaudhuri. 2008. “An N-Terminal Inhibitory Domain Modulates Activity of FoxM1 during Cell Cycle.” *Oncogene* 27 (12): 1696–1704.

Radhakrishnan, Ishwar, Gabriela C. Pérez-Alvarado, David Parker, H. Jane Dyson, Marc R. Montminy, and Peter E. Wright. 1997. “Solution Structure of the KIX Domain of CBP Bound to the Transactivation Domain of CREB: A Model for Activator:Coactivator Interactions.” *Cell* 91 (6): 741–52.

Radhakrishnan, Senthil K., Uppoor G. Bhat, Douglas E. Hughes, I-Ching Wang, Robert H. Costa, and Andrei L. Gartel. 2006. “Identification of a Chemical Inhibitor of the Oncogenic Transcription Factor Forkhead Box M1.” *Cancer Research* 66 (19): 9731–35.

Ramsay, Robert G., and Thomas J. Gonda. 2008. “MYB Function in Normal and Cancer Cells.” *Nature Reviews Cancer* 8 (7): 523–34.

Rossi, Paolo, Youlin Xia, Nandish Khanra, Gianluigi Veglia, and Charalampos G. Kalodimos. 2016. “15N and 13C- SOFAST-HMQC Editing Enhances 3D-NOESY Sensitivity in Highly Deuterated, Selectively [1H,13C]-Labeled Proteins.” *Journal of Biomolecular NMR* 66 (4): 259–71.

Rubin, Seth M. 2013. “Deciphering the Retinoblastoma Protein Phosphorylation Code.” *Trends in Biochemical Sciences* 38 (1): 12–19.

Shen, Yang, and Ad Bax. 2015. “Protein Structural Information Derived from NMR Chemical Shift with the Neural Network Program TALOS-N.” In *Artificial Neural Networks*, edited by Hugh Cartwright, 17–32. Methods in Molecular Biology. New York, NY: Springer New York.

Shen, Yang, Frank Delaglio, Gabriel Cornilescu, and Ad Bax. 2009. “TALOS+: A Hybrid Method for Predicting Protein Backbone Torsion Angles from NMR Chemical Shifts.” *Journal of Biomolecular NMR* 44 (4): 213–23.

Shi, Y, P E Kroeger, and R I Morimoto. 1995. “The Carboxyl-Terminal Transactivation Domain of Heat Shock Factor 1 Is Negatively Regulated and Stress Responsive.” *Molecular and Cellular Biology* 15 (8): 4309–18.

Spengler, Mary L., and Michael G. Brattain. 2006. “Sumoylation Inhibits Cleavage of Sp1 N-Terminal Negative Regulatory Domain and Inhibits Sp1-Dependent Transcription.” *Journal of Biological Chemistry* 281 (9): 5567–74.

Tugarinov, Vitali, and Lewis E. Kay. 2003. “Ile, Leu, and Val Methyl Assignments of the 723-Residue Malate Synthase G Using a New Labeling Strategy and Novel NMR Methods.” *Journal of the American Chemical Society* 125 (45): 13868–78.

Tyka, Michael D., Daniel A. Keedy, Ingemar André, Frank DiMaio, Yifan Song, David C. Richardson, Jane S. Richardson, and David Baker. 2011. “Alternate States of Proteins Revealed by Detailed Energy Landscape Mapping.” *Journal of Molecular Biology* 405 (2): 607–18.

Wang, F., C. B. Marshall, K. Yamamoto, G.-Y. Li, G. M. C. Gasmi-Seabrook, H. Okada, T. W. Mak, and M. Ikura. 2012. “Structures of KIX Domain of CBP in Complex with Two FOXO3a Transactivation Domains Reveal Promiscuity and Plasticity in Coactivator Recruitment.” *Proceedings of the National Academy of Sciences* 109 (16): 6078–83.

Wang, Xianxi, Anthony Arceci, Kelly Bird, Christine A. Mills, Rajarshi Choudhury, Jennifer L. Kernan, Chunxiao Zhou, Victoria Bae-Jump, Albert Bowers, and Michael J. Emanuele. 2017. “VprBP/DCAF1 Regulates the Degradation and Nonproteolytic Activation of the Cell Cycle Transcription Factor FoxM1.” *Molecular and Cellular Biology* 37 (13): e00609-16.

Wierstra, Inken, and Jürgen Alves. 2006. “Despite Its Strong Transactivation Domain, Transcription Factor FOXM1c Is Kept Almost Inactive by Two Different Inhibitory Domains.” *Biological Chemistry* 387 (7): 963–76.

Wright, Peter E., and H. Jane Dyson. 2015. “Intrinsically Disordered Proteins in Cellular Signalling and Regulation.” *Nature Reviews Molecular Cell Biology* 16 (1): 18–29.

Zor, Tsaffrir, Roberto N. De Guzman, H.Jane Dyson, and Peter E. Wright. 2004. “Solution Structure of the KIX Domain of CBP Bound to the Transactivation Domain of C-Myb.” *Journal of Molecular Biology* 337 (3): 521–34.